

Supporting Information for

Star-shape non-fullerene acceptor featuring an aza-triangulene core for organic solar cells

Yann Kervella,^a José Maria Andres Castán,^a Yatzil Alejandra Avalos-Quiroz,^b Anass Khodr,^b Quentin Eynaud,^b Tomoyuki Koganezawa,^c Noriyuki Yoshimoto,^d Olivier Margeat,^b Antonio J. Riquelme,^a Valid Mwatati Mwalukuku,^a Jacques Pécaut,^a Benjamin Grévin,^a Christine Videlot-Ackermann,^b Jörg Ackermann,^b Renaud Demadrille^a and Cyril Aumaitre^{a*}

^aIRIG-SyMMES, Université Grenoble Alpes/CEA/CNRS, Grenoble 38000, France
Mail :cyril.aumaitre@cea.fr

^bAix Marseille Univ, CNRS, CINAM, Marseille, France

^cIndustrial Application Division, Japan Synchrotron Radiation Research Institute (JASRI), Sayo, Hyogo 679-5198, Japan.

^dDepartment of Physical Science and Materials Engineering, Iwate University, Ueda Morioka 020 8551, Japan.

Email: C.A. (cyril.aumaitre@cea.fr)

Summary

| | | |
|------|--|----|
| I. | General information..... | 3 |
| | Materials | 3 |
| | Electrochemical characterization..... | 3 |
| | Theoretical calculations | 3 |
| | Film preparation and photodegradation measurements..... | 3 |
| | Solar cells fabrication and I-V measurement..... | 4 |
| | Thin film transistor fabrication and characterization..... | 4 |
| | Space Charge Limited Current (SCLC)..... | 4 |
| | Photovoltaic characterization..... | 5 |
| II. | Supplementary figures | 6 |
| III. | Impedance spectroscopy | 13 |
| | Experimental section | 13 |
| IV. | Degradation studies | 15 |
| V. | Synthesis | 18 |
| | 1. Synthesis of the precursors: | 18 |
| | 2. Synthesis of the NFA : | 20 |
| VI. | Xray Crystallographic structure datas | 29 |

I. General information

Materials

All chemical reactions were conducted in oven-dried or flame-dried glassware. The solvents, such as anhydrous toluene, chloroform and acetonitrile from Aldrich or Acros Organics were used as received. THF was used after distillation under sodium and benzophenone. All the starting materials were purchased from Sigma-Aldrich, Acros Organics or TCI chemicals and used as received. PTB7-Th and ITIC-Th were purchased from 1-materials. O-xylene, chlorobenzene (CB) and 1-chloronaphtalene (CN) were purchased from Sigma Aldrich, while ZnO 2.5% solution was obtained from Avantama.

Electrochemical characterization

Cyclic voltammetry measurements was carried out in a three-electrode electrochemical cell equipped with a flat platinum working electrode (7 mm²), a platinum-made counter electrode and an Ag/AgNO₃ reference electrode. The potentials were calibrated using the Fc⁺/Fc couple as an internal standard before and after each measurement, assuming this value to be -5.1 eV. The electrolyte consisted of a 0.1 M tetrabutylammonium hexafluorophosphate (Bu₄NPF₆) solution in anhydrous and degassed dichloromethane using a dye concentration of 10⁻³ M. The scanning rate was 100 mV/s.

Theoretical calculations

The geometry optimization was carried out using the ADF modeling suite 2016 software with a revPBE GGA functional corrected for dispersion using Grimme 3 methodology with TZ2P sets. The orbital simulation was eventually carried out using a single-point modeling with a B3LYP hybrid functional + dispersion and TZ2P sets in a COSMO model for PCM dichloromethane on the previously optimized geometries. Time-Dependent DFT calculations was performed with ADF to estimate the electronic excitations. Only singlet allowed transitions was chosen, and ten roots were evaluated. A PBE0 hybrid functional was investigated together with TZ2P basis sets. The solvent (chloroform) was taken into account as a polarizable model. The spectra was displayed using the ADF Graphical User Interface.

Film preparation and photodegradation measurements.

To prepare neat materials solutions, 10 mg/ml of donor polymer (PTB7-Th) and 20 mg/ml of acceptors were dissolved in chlorobenzene or in o-xylene and stirred overnight at 60°C. For stability test, the neat solutions are then spin-coated on top of cleaned glass and KBr transparent substrates, the films are subsequently annealed at 100°C for 10 min to eliminate solvent. Then all the films were place in a sample holder that allowed measuring the same spot in the film during characterization. Half of the films were sealed under inert conditions in a glass tube under vacuum (photolysis), the rest were keep as prepared in presence of oxygen (photo-oxidation). Photodegradation experiments were performed in a SUNTEST CPS/XLS Atlas device designed to simulate the AM1.5 spectrum. UV light below 400 nm were cut off with an industrial UV filter. The black standard temperature was set at 60°C, which corresponds to a chamber temperature of around 35°C. Irradiation provided by a xenon lamp from Atlas (NXE1700) was set at 1000 W/m² in the UV-visible domain. The films were characterized before degradation and at different time periods during illumination. UV-visible spectra were obtained on a Shimadzu UV-2600 spectrophotometer equipped with an integrating sphere. The absorbance of the samples was measured and integrated in the 200-1000 nm range. Infrared transmission spectra were recorded with a Thermo Scientific Nicolet 6700 spectrophotometer purged with dry air (32 acquisitions summation with 4 cm⁻¹ resolution). The sample holder used for the films allowed measuring the same spot in the film.

Solar cells fabrication and I-V measurement.

PTB7-Th:AzaTrk inks were prepared in chlorobenzene (97% CB/3% CN) or in *o*-xylene in a total concentration of 20 mg/ml in ratio 1:1 and stirred at 60°C overnight. ITO-coated glass (sheet resistance 10-15 Ω/square) purchased from LUMTEC were sequentially cleaned with deionized water, acetone and isopropanol under sonication for 15 min each, dried with argon and then treated in a UV-ozone oven for 15 min at 80°C. All the devices were fabricated in inverted structure ITO/ZnO/Active Layer/MoO₃/Ag. ZnO layer was spin-coated in air from a 1% v/v solution in isopropanol at 5000 rpm follow by thermal annealing at 120°C for 10 min. The substrates were then transferred to a N₂-filled glovebox where a blend film of 45-72 nm thickness was spin-coated at 1500 rpm during 2 min on top of ZnO films. At this stage of solar cell fabrication, a thermal annealing was applied at 80°C for 5 min. Finally, 5 nm MoO₃ and 100 nm Ag were deposited by thermal evaporation through a mask to define an active area of 0.16 cm². The current density-voltage characterization of the devices under AM1.5G light solar simulator (Newport Sol3A Class AAA) were recorded with a Keithley 238 source meter unit inside the glove box. The illumination intensity of the light source was calibrated to be 100 mW/cm² using a standard silicon solar cell (Newport Company, Oriel no. 94043A) calibrated by the National Renewable Energy Laboratory (NREL). The EQE of the solar cells was measured using a 150 W Xenon arc lamp along with Oriel Cornerstone 260 monochromator.

Thin film transistor fabrication and characterization.

Interdigitated TFT structures were purchased from Fraunhofer (Germany) with n-doped silicon wafers covered with thermally grown silicon dioxide (SiO₂) followed by a lift-off deposited source and drain electrodes composed of 10 nm of indium tin oxide (ITO) and 30 nm of gold (Au). Channel length *L* to channel width *W* ratios were 20/10000 μm or 10/10000 μm. Prior the deposition of the NFA-based solutions by spin-coating, the substrates were first cleaned. Both electrodes and SiO₂ dielectric surfaces were chemically modified with a thiol derivative, namely 4-(dimethylamino) benzenethiol (DABT) and divinyl-tetramethyldisiloxane-bis(benzocyclobutene (BCB), respectively.^[1,2] AzaTrk solutions were prepared in chlorobenzene or *o*-xylene at a concentration of 10 mg/ml and stirred overnight at 60°C for chlorobenzene and room temperature for *o*-xylene. Solutions were spin-coated at 1000 rpm during 2 minutes with a spin-coater machine from SET Company (model TP 6000) on top of the source and drain electrodes in nitrogen-filled glove box. OTFTs were annealed on a preheated hot plate at 150°C or 200°C for 10 min as a post-treatment. Current-voltage characteristics were performed with a Hewlett-Packard 4140B pico-amperemeter-DC voltage source. The mobility values μ were extracted from the saturation region of the transfer curves with the equation: $I_D = W/2L C_{ox} \mu (V_G - V_T)^2$ where I_D is the drain-source current, C_{ox} is the capacitance per unit area of the gate insulator layer ($C_{ox} = 18.8 \times 10^{-9}$ F.cm⁻²), V_G is the gate voltage, V_T is the threshold voltage, and μ is the field-effect mobility. All electrical characterization results were performed in nitrogen-filled glove box.

Space Charge Limited Current (SCLC).

SCLC devices require careful choice of the contacts to ensure sufficient injection of the desired carrier, and effective blocking of the other carrier to work like single-carrier devices.^[3] Hole-only and electron-only devices consisted of ITO/PEDOT:PSS/PTB7-Th:AzaTrk/MoO_x/Au and ITO/ZnO/PTB7-Th:AzaTrk/LiF/Al, respectively. ZnO was deposited as OPV devices. Top metallic electrodes were thermally evaporated (MBRAUN evaporator) at 2×10^{-6} Torr to a controlled thickness (13 nm of MoO_x, 100 nm Au, 0.5 nm LiF and 100 nm of Al) using a shadow mask that defines the device areas to 0.09 cm² or 0.25 cm² and allows a four-point measurement. The pristine PTB7-Th:AzaTrk solutions were deposited by spin-coating at 600 or 800 rpm for 120 sec for *o*-xylene and CB (97% CB/3% CN), respectively. Active layers were subsequently annealed at 80°C during 5 minutes. The thicknesses of thin films were measured precisely with a Veeco Dektak 150 (Table S2).

The measured dark current was fitted using the Murgatroyd expression:

$$I = A\mu_0 \frac{9V^2}{8d^3} \varepsilon\varepsilon_0 \exp\left[-\frac{0.891\gamma}{\sqrt{d}}\right] \quad (1)$$

where d is the active layer thickness, A is the active device area, $\varepsilon\varepsilon_0$ is the permittivity of the active layer (ε is assumed equal to 3.5 and ε_0 is the permittivity of free space), and V is the voltage. μ_0 and γ are the unknown parameters that will be adjusted to get a good fit, all other parameters are fixed. μ_0 is the mobility at low electric fields, and γ is a parameter that represents the field dependence of mobility.

Photovoltaic characterization.

The current density–voltage (J–V) characteristics of the devices were measured using a Keithley 238 Source Measure Unit inside the glove box. Solar cell performance was measured using a Newport class AAA 1.5 Global solar simulator (Oriel Sol3ATM model no. 94043A) with an irradiation intensity of 100 mW cm⁻². The light intensity was determined with a Si reference cell (Newport Company, Oriel no. 94043A) calibrated by the National Renewable Energy Laboratory (NREL).

Thin films characterization.

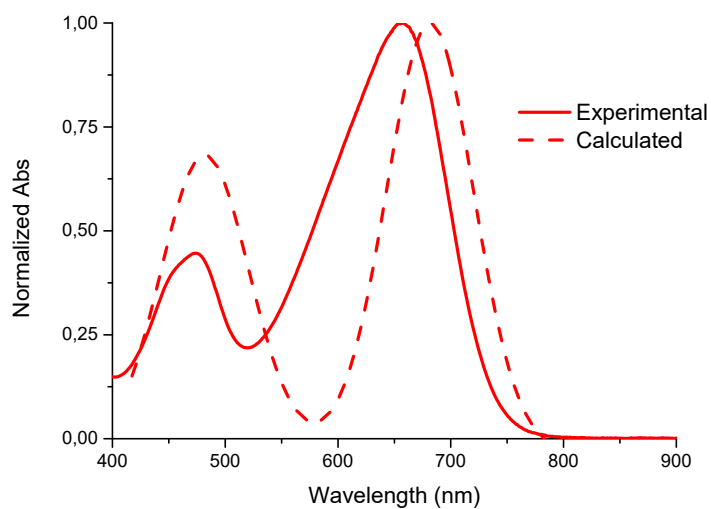
The absorbance of the active layer films was measured by UV–Vis–near infra-red Spectrophotometer Cary 5000. The surface morphology of the blend layers was investigated by AFM (NTEGRA from NT-MIDT) in tapping mode using the silicon tips (MikroMash) with a theoretical resonant frequency of 300 kHz and a spring constant of 16 N m⁻¹ at room temperature. Film thicknesses were measured by a stylus profilometer (Bruker DEKTAK XT) with a 1 mg force on the probing tip.

Thin films were further analyzed by 2D grazing-incidence X-ray diffractometry (2D-GIXRD) with high-brightness synchrotron radiation at BL19B2 in SPring-8 (Japan). 2D-GIXRD measurements were performed using a high-sensitive 2D X-ray detector (PILATUS 300K). The incident angle and wavelength of X-rays were 0.13° and 0.100 nm, respectively. The crystal coherence length (CCL) values were extracted by the Scherrer equation from FWHM:

$$\tau = \frac{K\lambda}{\beta \cos\theta} \quad (2)$$

where τ is the ordered (crystalline) domains mean size, here defined as CCL, K is a constant (dimensionless shape factor) closed to unity. The shape factor is typically equal to 0.9, λ is the wavelength of the X-ray, β is the FWHM of the diffraction peak after subtracting the instrumental line broadening and θ is the Bragg angle.

II. Supplementary figures



| Wavelength (nm) | Oscillator strength | Transition |
|-----------------|---------------------|--|
| 684 | 1.42 | HOMO->LUMO (94.9%) |
| 679 | 1.68 | HOMO->LUMO (94.8%) |
| 481 | 1.26 | HOMO-1->LUMO (71.2%) HOMO-1->LUMO+1 (13.8%) |
| 478 | 0.50 | HOMO-1->LUMO (64.0%) HOMO->LUMO+2 (18.6%) HOMO-1->LUMO+1 (11.1%) |

Figure S 1 – Experimental and calculated absorption spectra of AzaTk and attribution of the optical bands to the electronic transition.

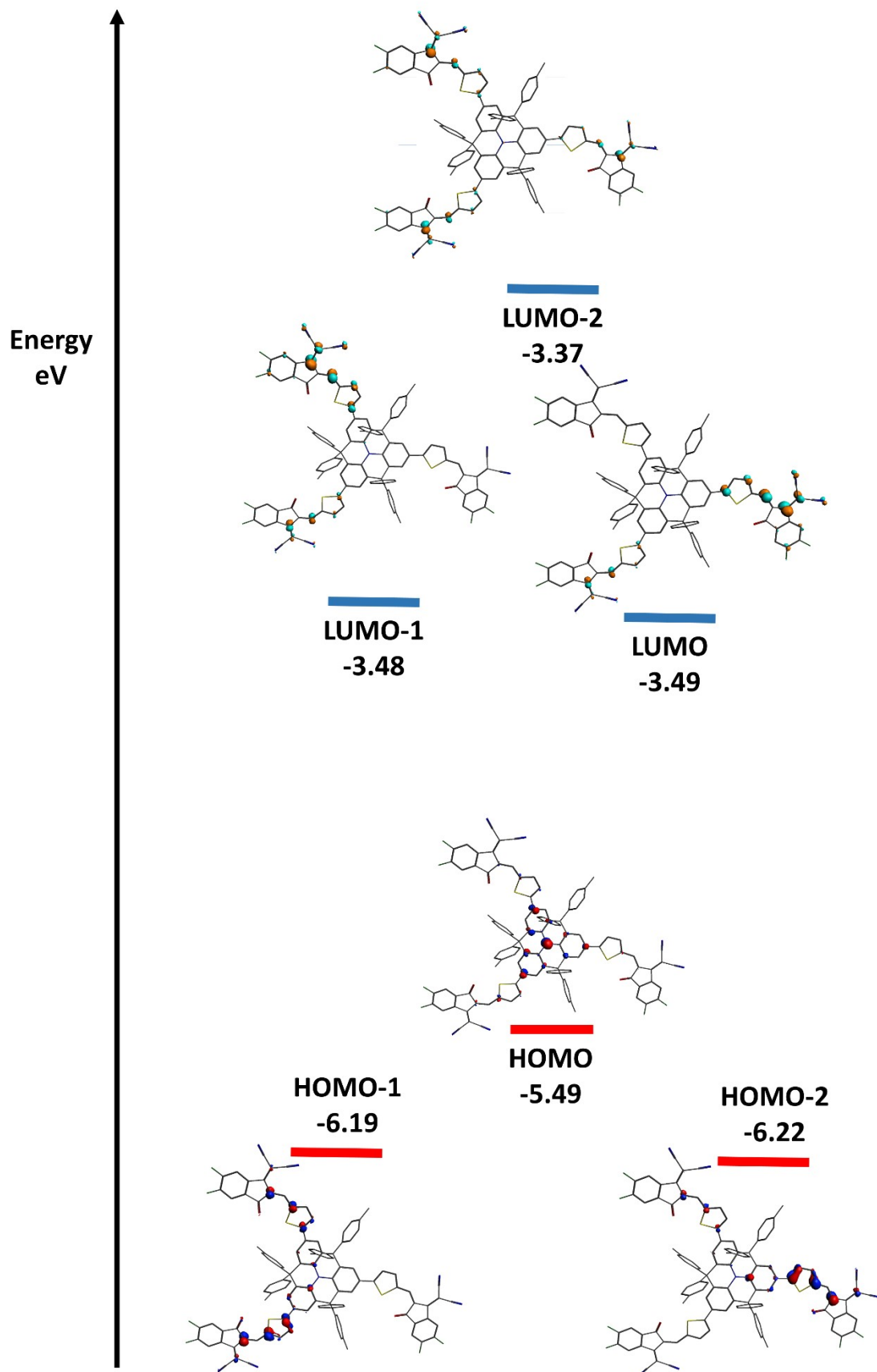


Figure S 2 – Representation of the electronic density localization on several AzaTk frontiers orbitals.

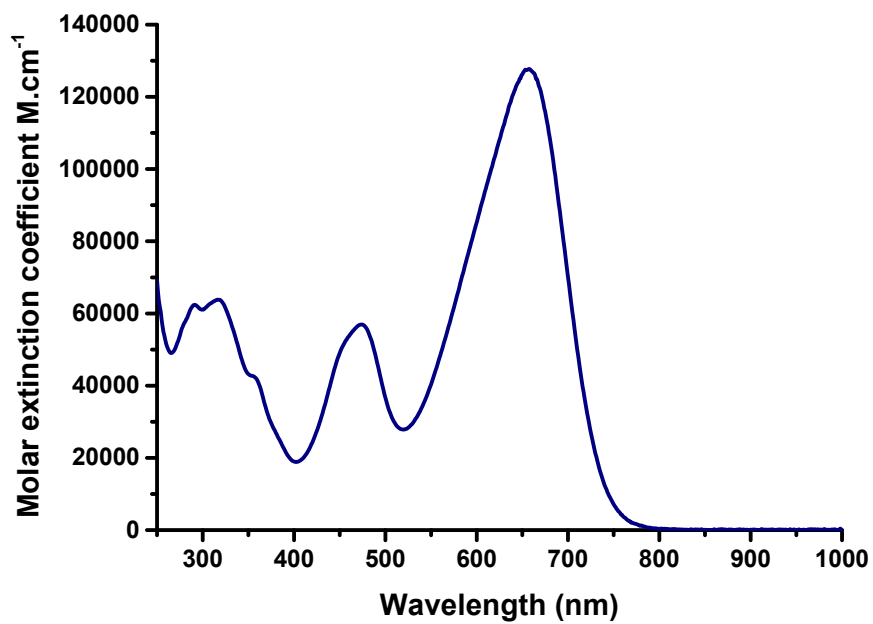


Figure S 3 - Absorption spectrum of AzaTk in chloroform solution (10^{-5} M) vs. molar extinction coefficient

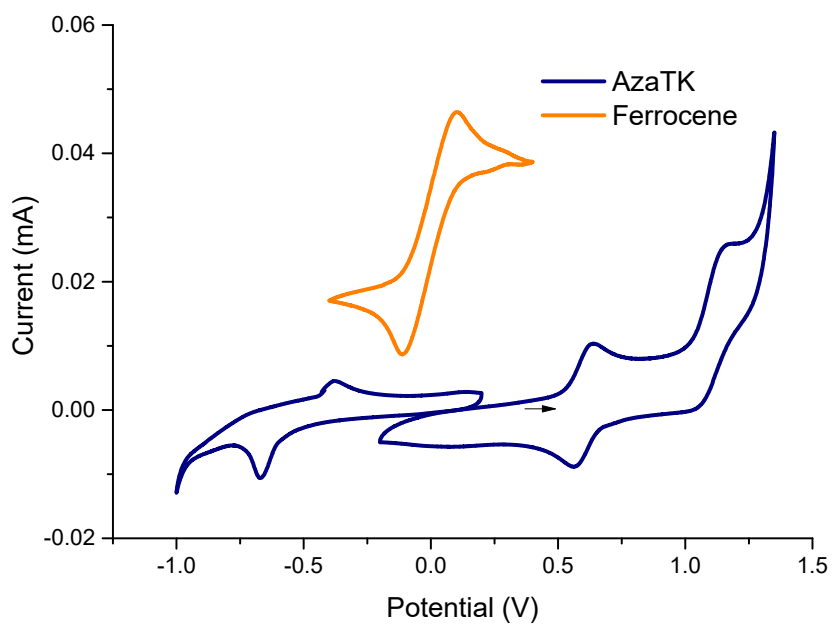


Figure S 4 - Cyclic voltammogram of AzaTk in dichloromethane with Ag/AgNO₃ as reference electrode and Fc/Fc⁺ couple as an internal reference.

| Compound | μ_{electron} ($\text{cm}^2 \cdot \text{V}^{-1} \cdot \text{s}^{-1}$) | V_T (V) | Solvent | Annealing |
|------------------------|--|------------------|---------------|-----------|
| AzaTrk | $1.13 \pm 0.11 \times 10^{-4}$ | 20.19 ± 3.70 | O-Xylene | as-cast |
| | $1.99 \pm 0.25 \times 10^{-4}$ | 20.53 ± 3.70 | | 150°C |
| | $2.15 \pm 0.45 \times 10^{-4}$ | 28.50 ± 1.89 | | 200°C |
| | $1.23 \pm 0.85 \times 10^{-4}$ | 10.55 ± 1.25 | Chlorobenzene | as-cast |
| | $1.42 \pm 0.78 \times 10^{-4}$ | 10.64 ± 1.10 | | 150°C |
| | $2.70 \pm 0.42 \times 10^{-4}$ | 12 ± 1.31 | | 200°C |
| ITIC-Th ^[1] | $5.5 \pm 2 \times 10^{-3}$ | 17.6 ± 7.7 | Chlorobenzene | as-cast |
| | $5.9 \pm 1 \times 10^{-3}$ | 22.4 ± 5.1 | | 120°C |
| | $1.3 \pm 2 \times 10^{-3}$ | 15.2 ± 4.9 | | 150°C |
| | $4.5 \pm 1.5 \times 10^{-3}$ | 17.8 ± 4.5 | | 200°C |

Table S 1 - . Electron transport parameters of AzaTrk and ITIC-Th molecules evaluated in BGBC OTFTs for as-cast and post-annealed thin film. Molecules were dissolved in chlorobenzene or in O-xylene.

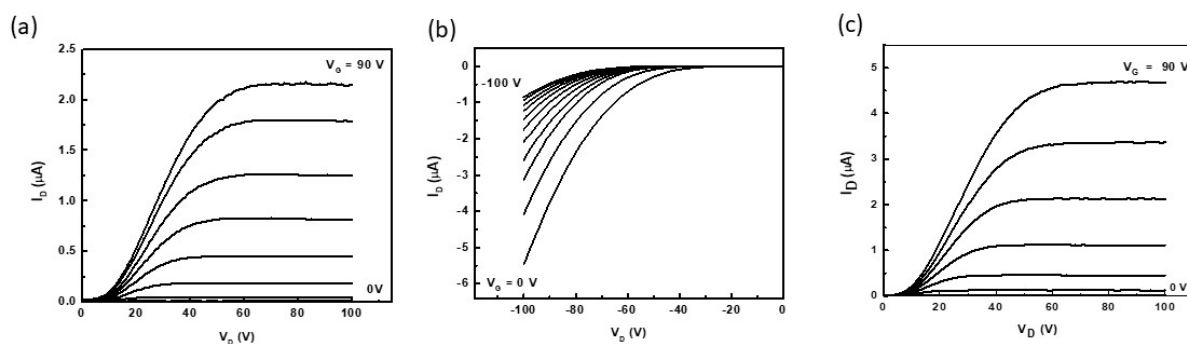


Figure S 5 - a) Output characteristics in the accumulation mode (under positive bias) and in the depletion mode (under negative bias) of a BGBC OTFT based on as-cast AzaTrk thin film from O-xylene. c) Output characteristics in the accumulation mode (under positive bias) of a BGBC OTFT based on 200°C post-annealed AzaTrk thin film from O-xylene.

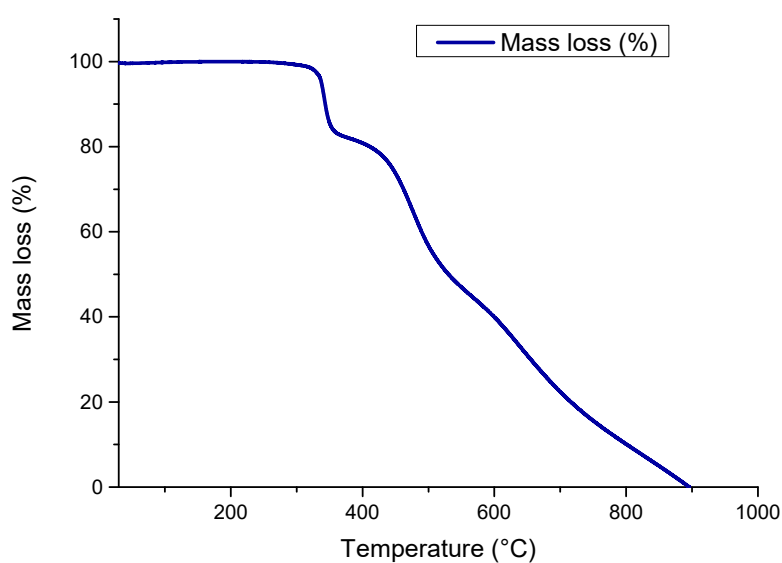


Figure S 6 - Thermal gravimetric analysis curve of AzaTrk molecule

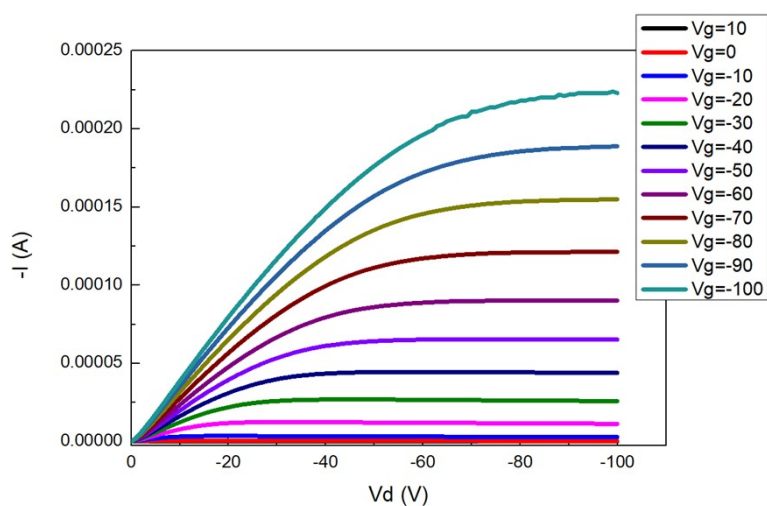


Figure S 7 - Output characteristics of a BGBC OTFT based on as-cast PTB7-Th (the accumulation mode under negative bias). Both SiO_2 dielectric layer and ITO/Au electrodes have not been treated to measure the holes transport in the donor PTB7-Th polymer.

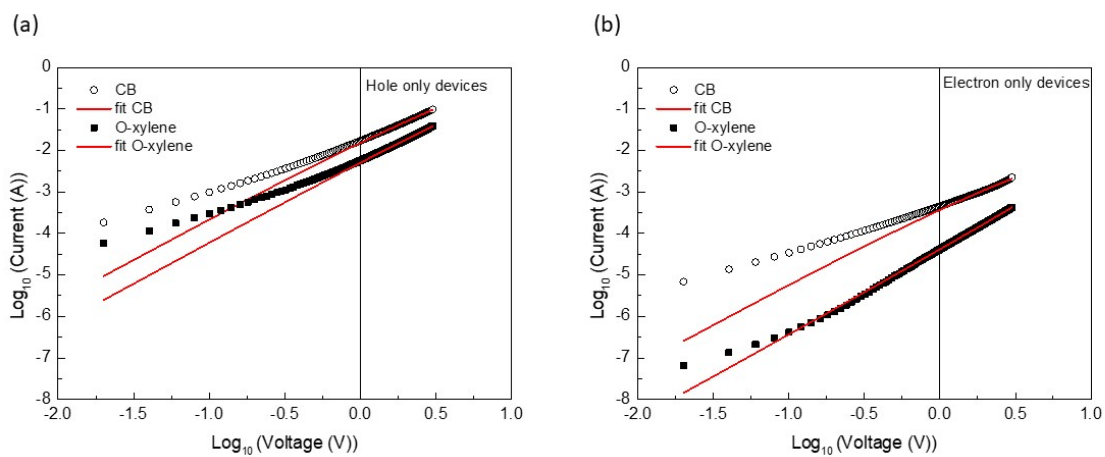


Figure S 8 - Current vs. voltage for holes (a) and electron (b) only devices based on PTB7-Th:AzaTrk blends with ratio 1:1 in chlorobenzene (CB) and o-xylene. The charges carrier mobility values of PTB7-Th:AzaTrk blends were determined following the single-carrier devices SCLC model.

| Solvent | Hole only devices | | Electron only devices | |
|----------|-------------------|--------------------------------|-----------------------|--------------------------------|
| | thickness d (nm) | μ_h (cm ² /V.s) | thickness d (nm) | μ_e (cm ² /V.s) |
| CB | 98 | 7.61x10 ⁻⁴ | 150 | 3.53x10 ⁻⁵ |
| | | 7.98x10 ⁻⁴ | | 5.77x10 ⁻⁵ |
| | | 7.58x10 ⁻⁴ | | 7.54x10 ⁻⁵ |
| | | 8.82x10 ⁻⁴ | | 8.82x10 ⁻⁶ |
| | | 8 x10⁻⁴ | | 6.54 x10⁻⁵ |
| O-xylene | 112 | 3.32x10 ⁻⁴ | 75 | 3.8x10 ⁻⁷ |
| | | 3.16x10 ⁻⁴ | | 1.72x10 ⁻⁶ |
| | | 2.82x10 ⁻⁴ | | 4.16x10 ⁻⁶ |
| | | | | 4.03x10 ⁻⁶ |
| | | 3.10 x10⁻⁴ | | 1.89 x10⁻⁶ |

Table S 2 - Hole (μ_h) and electron (μ_e) mobility values obtained by SCLC of PTB7-Th:AzaTrk bulk heterojunction layers as function of solvent. In grey, an average value is given for each configuration (hole/electron v.s. solvent) of devices.

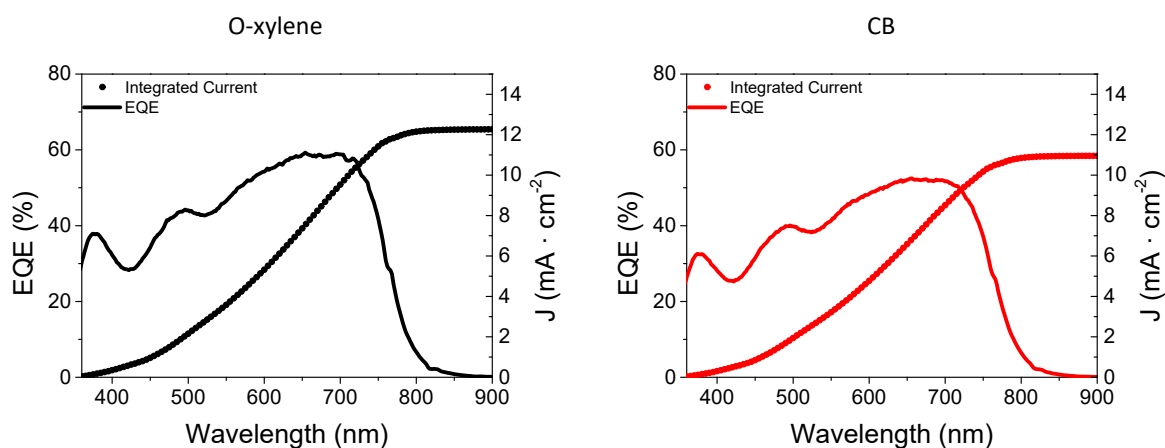


Figure S 9 - EQE spectrum and integration of the current density of PTB7-Th:AzaTrk blend layers in o-xylene and chlorobenzene in inverted solar cells structure.

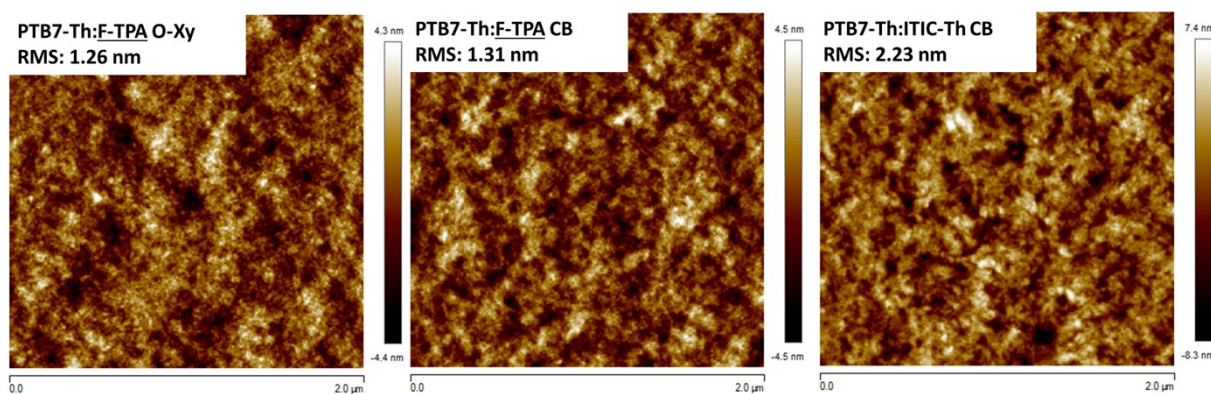


Figure S 10 AFM images of PTB7-Th:AzaTrk blend films from o-xylene and chlorobenzene solutions and PTB7-Th:ITIC-Th in chlorobenzene solution.

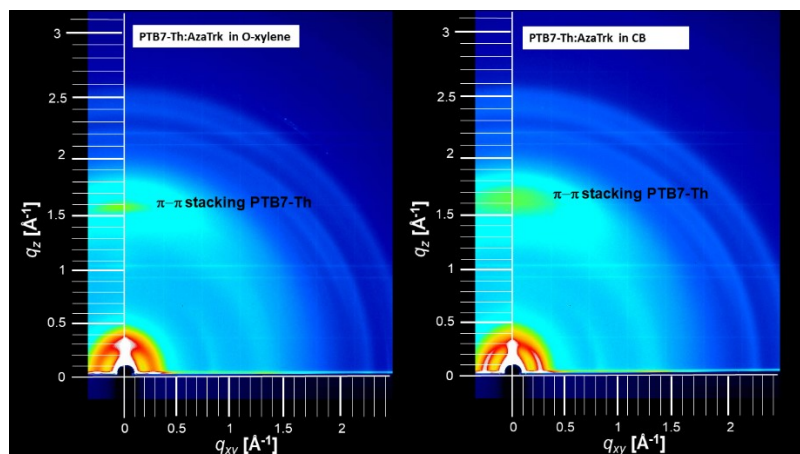


Figure S 11 2D-GIXRD patterns of PTB7-Th:AzaTrk (ratio d 1:1) blend layers deposited on ZnO buffer layer as function of solvent.

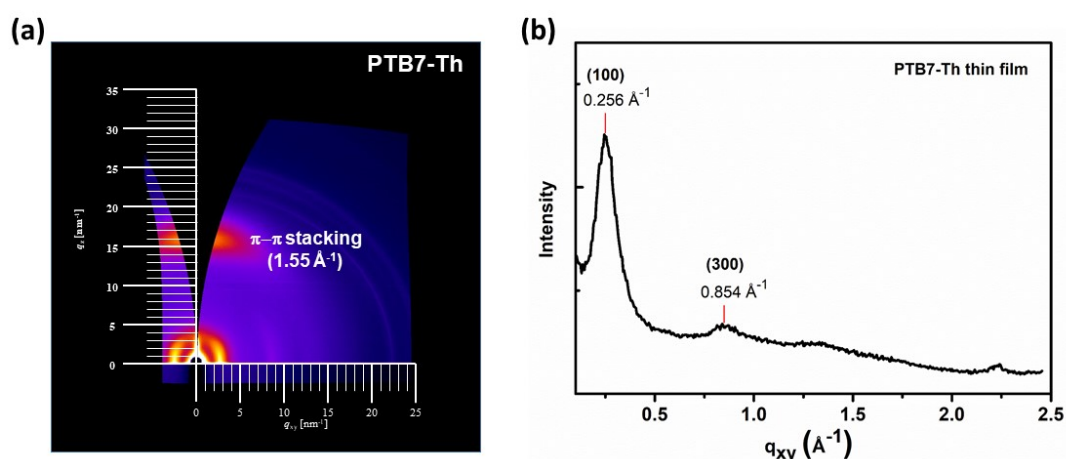


Figure S 12 2D-GIXRD patterns (a) and in plane of line cut (b) of a neat PTB7-Th layer deposited on ZnO buffer layer from CB solution.

III. Impedance spectroscopy

Experimental section

The electrochemical impedance spectroscopy (EIS) measurements were done using an Autolab PGSTAT30 FRA2 potentiostat controlled by the NOVA 2.1 software. These measurements were done using a white Thorlabs LED in a wide range of light intensities. The applied DC potential was equal to the generated open-circuit voltage under continuous illumination under each light intensity. The impedance spectra were obtained by applying a 10 mV sinusoidal perturbation superimposed to the DC applied voltage in the $10^5 - 100$ Hz frequency range. The resulting spectra were analysed and modelled using ZView software (Scribner).

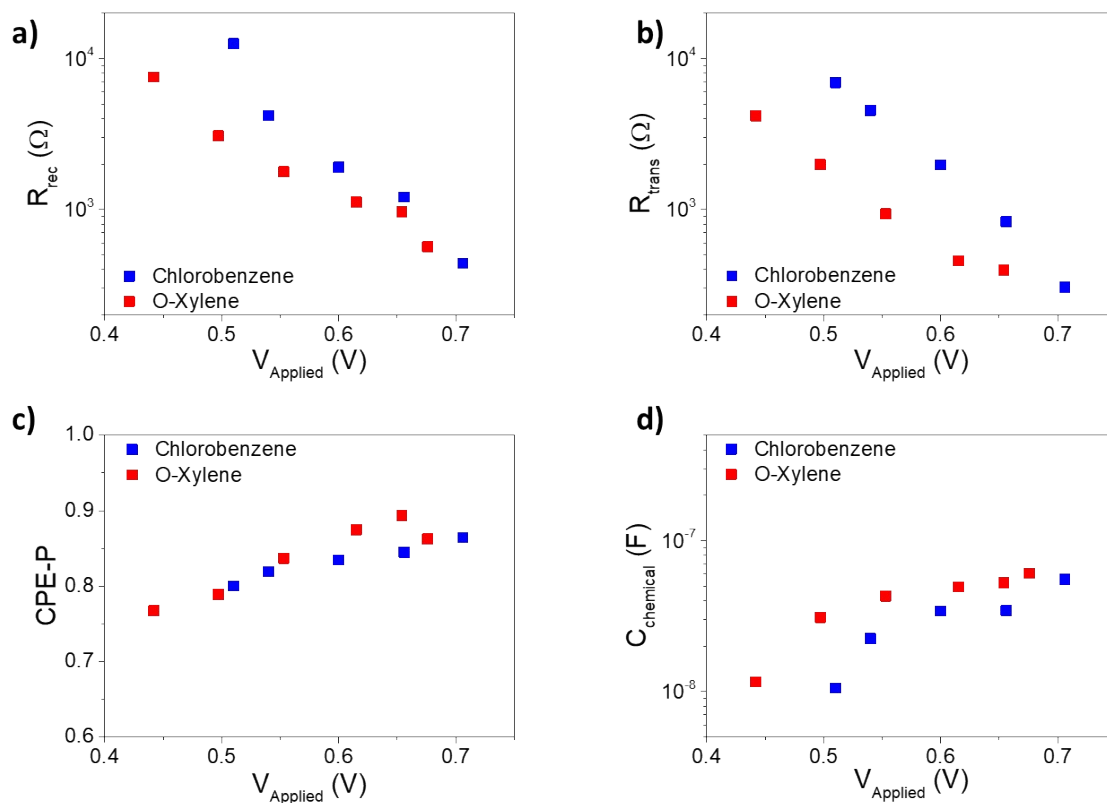


Figure S 13 Recombination resistance (a), transport resistance (b), CPE-P (c) and chemical capacitance (d) extracted from the impedance spectra of Azatriangulene-based organic solar cells using O-Xylene and Chlorobenzene as solvents under white illumination, applying the equivalent circuit depicted in the inset of figure 5 of main text.

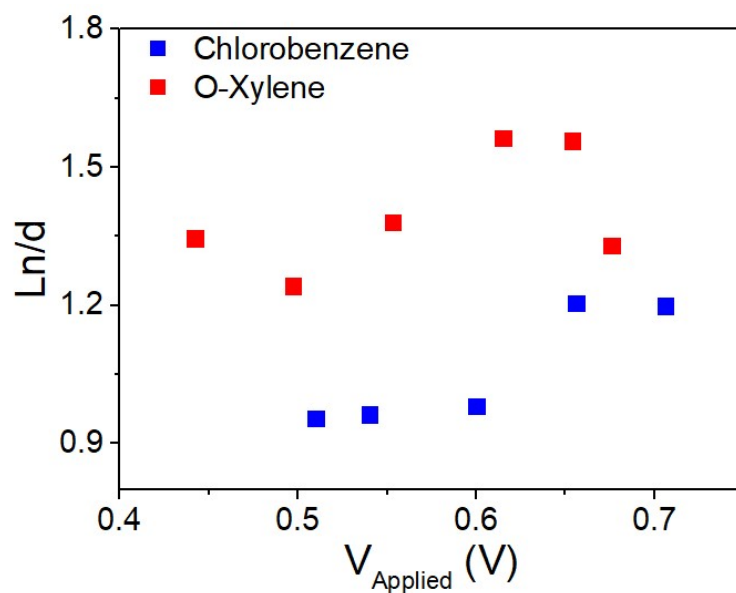


Figure S 14 Ratio between small perturbation diffusion length and active layer thickness, extracted from the impedance spectra of Azatriangulene-based organic solar cells using O-Xylene and Chlorobenzene as solvents under white illumination using Equation 1 from main text.

IV. Degradation studies

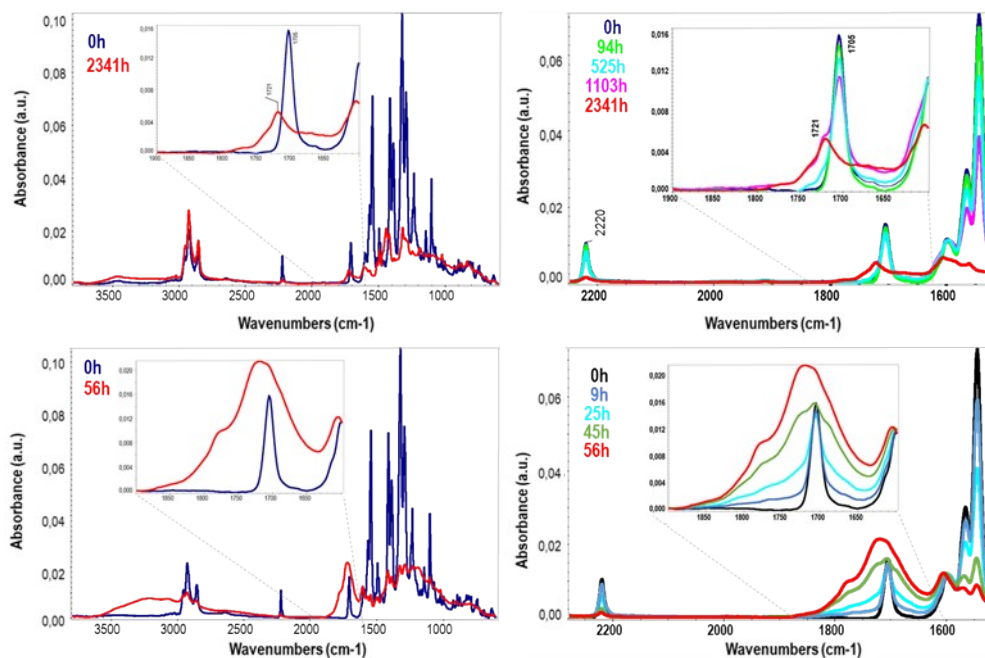


Figure S 15 IR spectra of AzaTk molecule under constant illumination using simulated AM1.5 light at 1000 W/m², 400 nm UV light filter and 35°C in a) absence of oxygen and b) presence of oxygen.

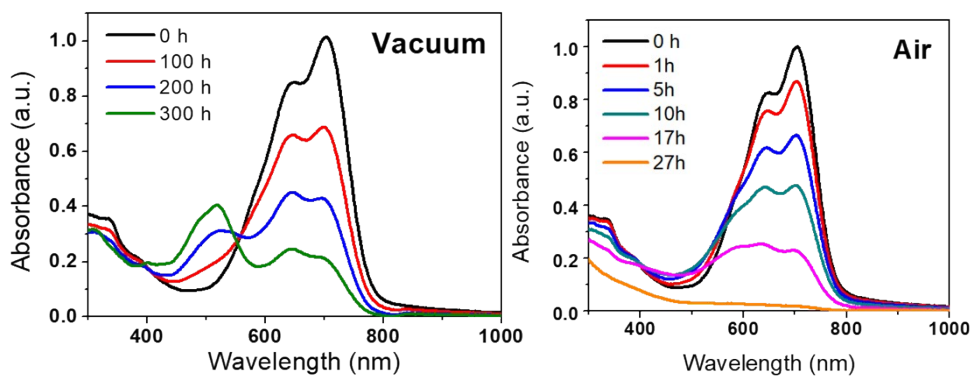


Figure S 16 Absorbance spectra of the evolution of ITIC molecule under constant illumination using simulated AM1.5 light in a) absence of oxygen (vacuum) and b) presence of oxygen (air)

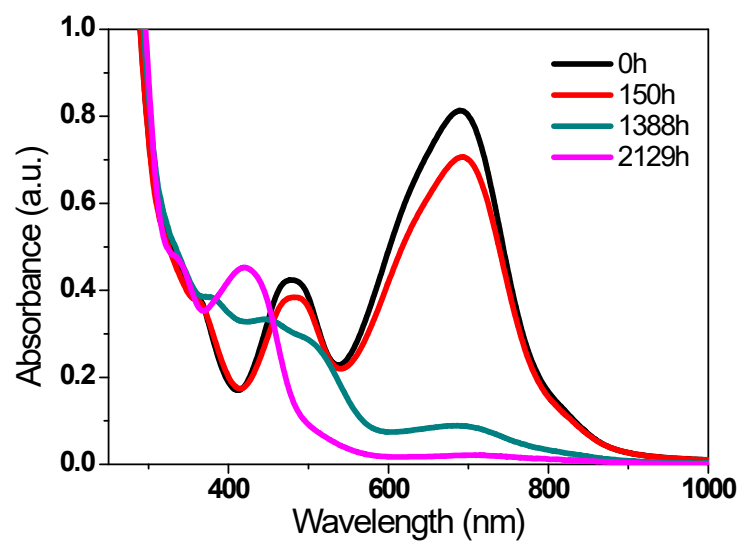


Figure S 17 Absorbance spectra of the evolution of AzaTk molecule film deposited on glass under constant illumination using simulated AM1.5 light in absence of oxygen (vacuum)

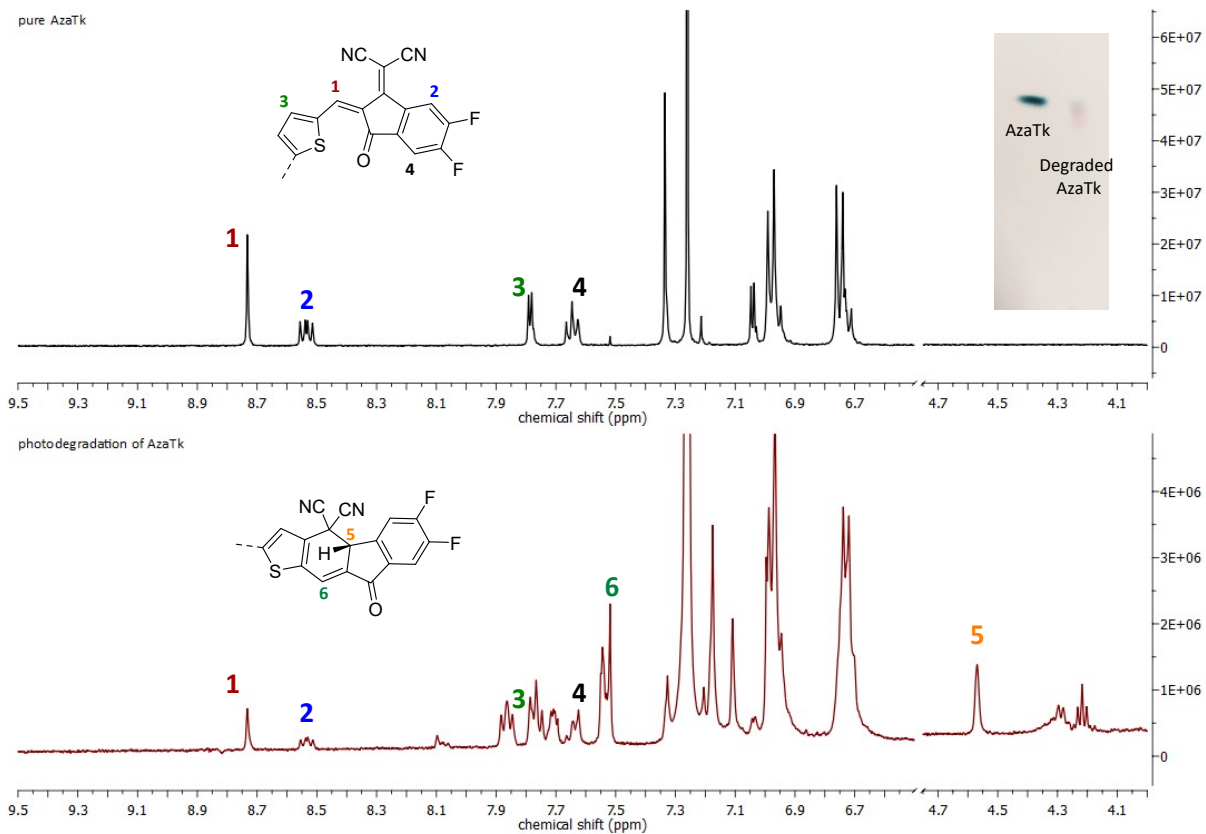


Figure S 18 – ^1H NMR spectra of pure AzaTk (top) and after photodegradation (bottom). Attribution of the peaks in correlation of Perepishka group.^[1]

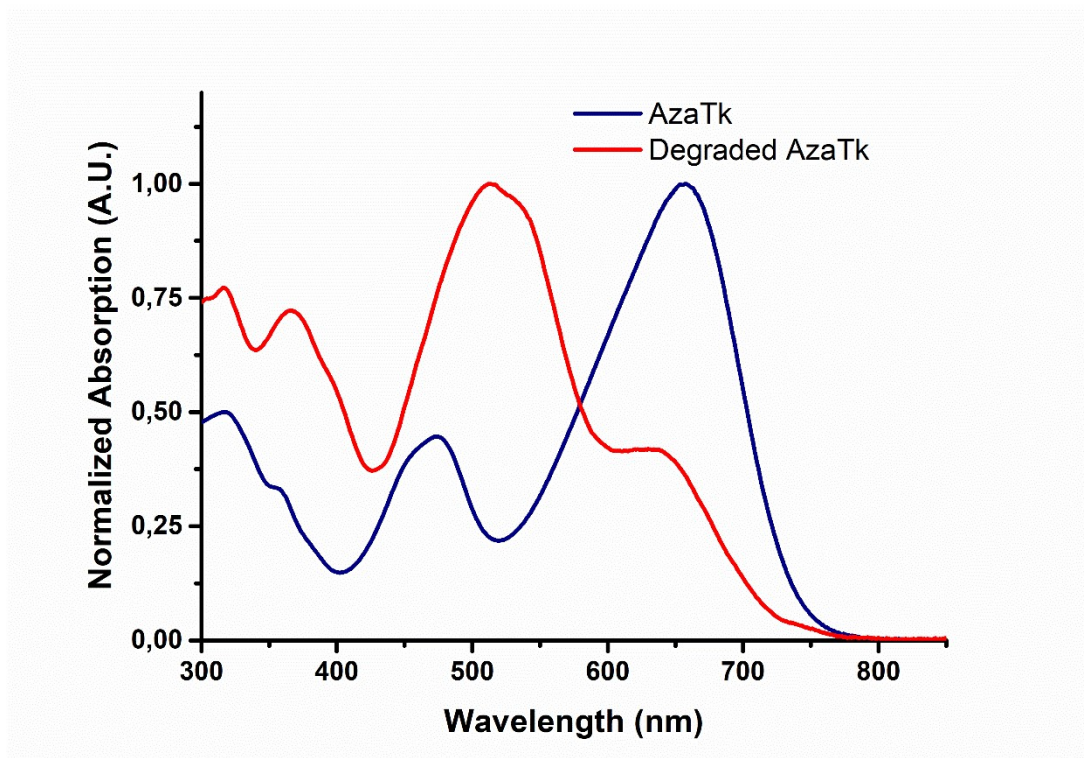
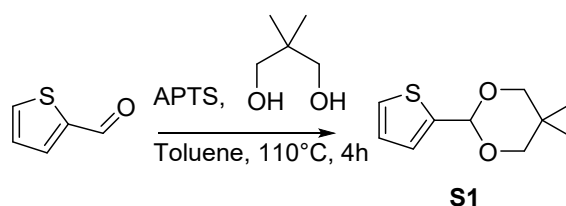


Figure S 19 – Absorption spectra of pure AzaTk and after photodegradation.

V. Synthesis

1. Synthesis of the precursors:



Synthesis of 5,5-dimethyl-2-(thiophen-2-yl)-1,3-dioxane (S1)

A dry round bottom flask was charged with thiophene-2-carbaldehyde (30.0 g, 0.27 mol), neopentylglycol (33.4 g, 0.32 mol, 1.2 eq) and *p*-toluenesulfonic acid (460 mg, 2.7 mmol, 1% mol). Then, 250mL of toluene were added and the mixture was stirred at 110°C for 4h. After cooling down, the crude was washed with water and the organic layer was dried with Na₂SO₄, filtered and evaporated in vacuum. The product was recrystallized from hexane affording the pure compound as a white solid (33.8 g, 0.17 mol, 63.7%).

¹H NMR (CDCl₃, 400 MHz, 298 K) : δ (ppm) = 7.30 (dd, *J* = 5.0, 1.2 Hz, 1H), 7.14 (ddd, *J* = 3.5, 1.2 Hz, 1H), 6.99 (dd, *J* = 5.0, 3.5 Hz, 1H), 5.65 (s, 1H), 3.76 (m, *J* = 10.0, 1.0 Hz, 3H), 3.64 (m, *J* = 10, 1.0 Hz, 3H), 1.29 (s, 3H), 0.80 (s, 3H).

¹³C NMR (CDCl₃, 100 MHz, 298 K) : δ (ppm) = 141.10, 126.16, 125.38, 124.78, 98.02, 29.91, 22.70, 21.55.

Anal. Calcd for C₁₀H₁₄O₂S: C, 60.57; H, 7.12; S, 16.17. Found: C, 60.79; H, 6.79; S, 16.29.

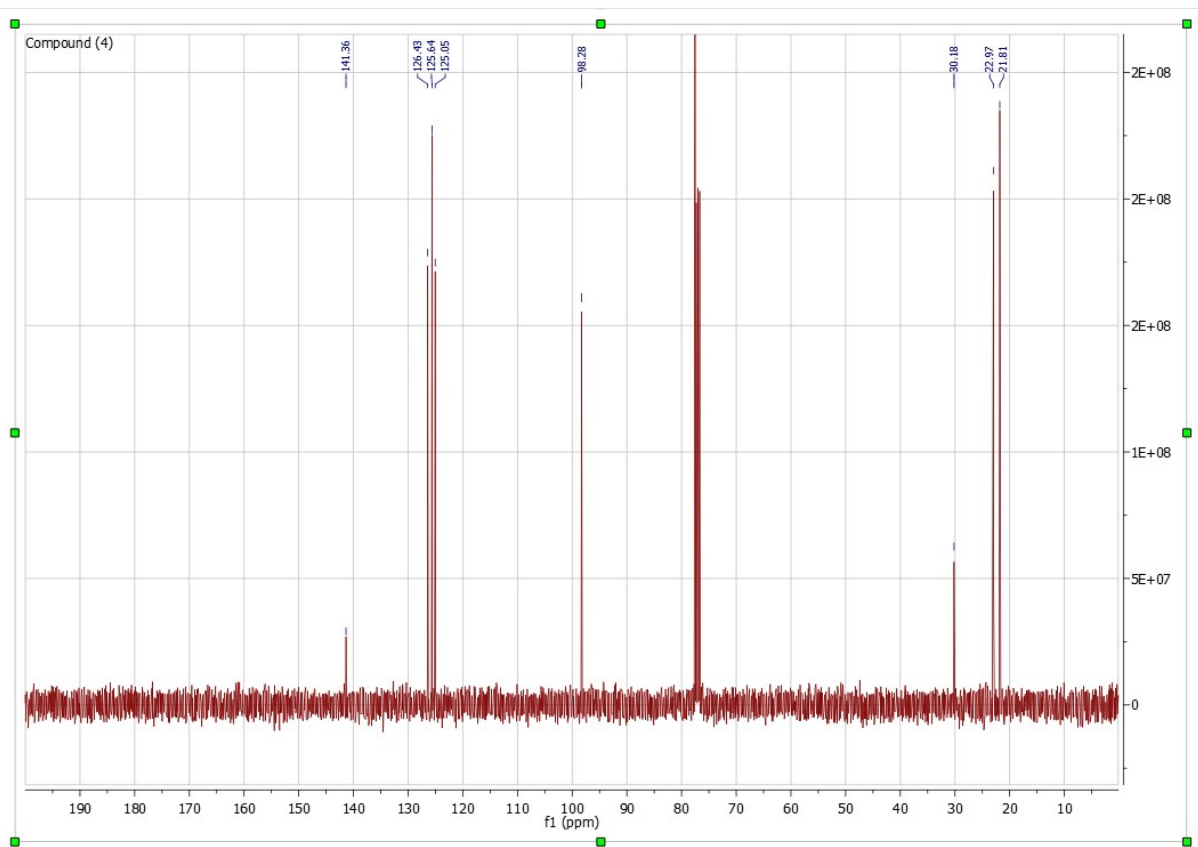
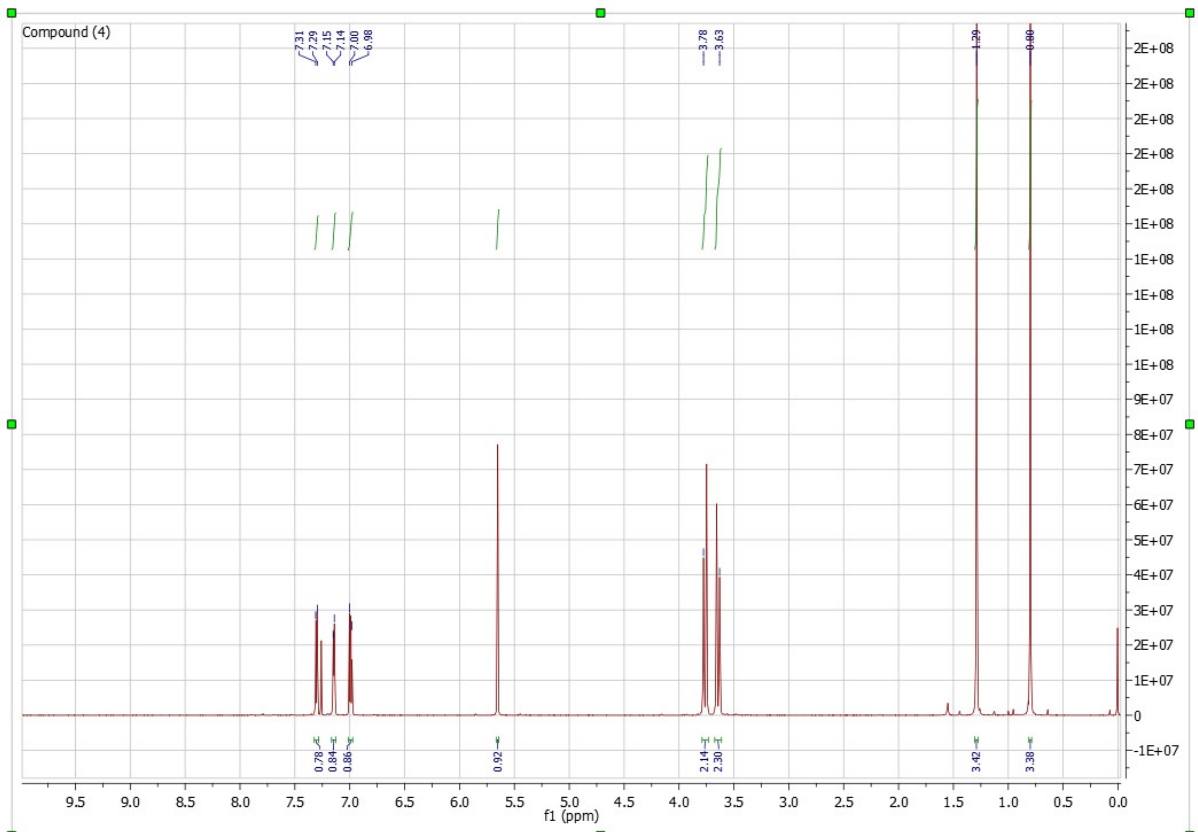
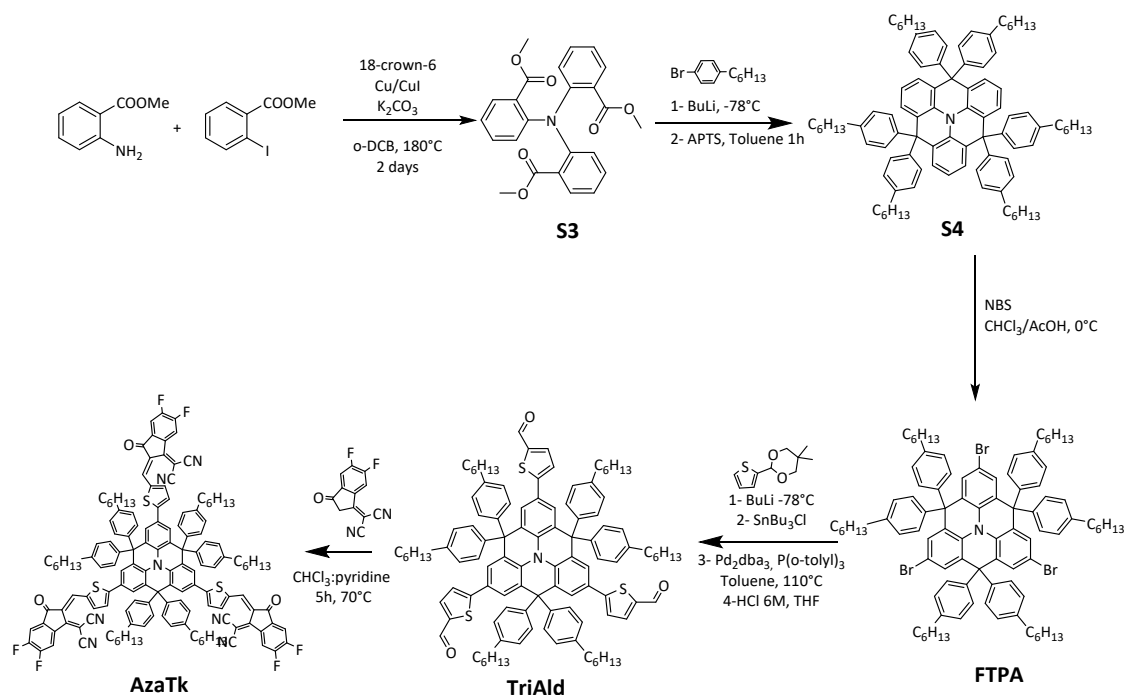


Figure S 20 - ^1H and ^{13}C NMR spectra of compound S1

2. Synthesis of the NFA :



Synthesis of trimethyl-2,2',2''-nitrilotribenzoate (S3)

Methyl 2-aminobenzoate (2.56 mL, 19.8 mmol, 1 eq.), methyl 2-iodobenzoate (11.7 mL, 79.4 mmol, 4 eq.), K₂CO₃ (7.13 g, 51.6 mmol, 2,6 eq.), Cu (0.252 g, 4 mmol, 20 mol%) and CuI (0.377 g, 2 mmol, 10 mol%), 18-crown-6 (0.786 mg, 3 mmol, 15 mol%) was dissolved in o-dichlorobenzene (50 mL) and was heated at 180 °C for 2 days. At room temperature, the reaction mixture was filtered on a celite pad, rinsed with dichloromethane. The organic layer was removed under reduced pressure and the crude product was dissolved with 50 mL of ethyl acetate and left at -20 °C overnight. After filtration and washing with ethyl acetate, we obtained the product **S3** as an off-white solid (4.43 g, 53.2 %).

¹H NMR (400 MHz, CDCl₃, 298 K) δ 7.61 – 7.58 (m, 3H); δ 7.38 – 7.33 (m, 3H); δ 7.10 – 7.04 (m, 6H); δ 3.37 (s, 3H).

¹³C NMR (400 MHz, CDCl₃, 298 K) δ 167.7, δ 146.9, δ 132.1, δ 130.9, δ 127.4, δ 123.5, δ 119.8, δ 51.6.

Anal. Calcd for C₂₅H₂₃NO₆: C, 69.27; H, 5.35; N, 3.23. Found: C, 69.10; H, 5.36; N, 3.16.

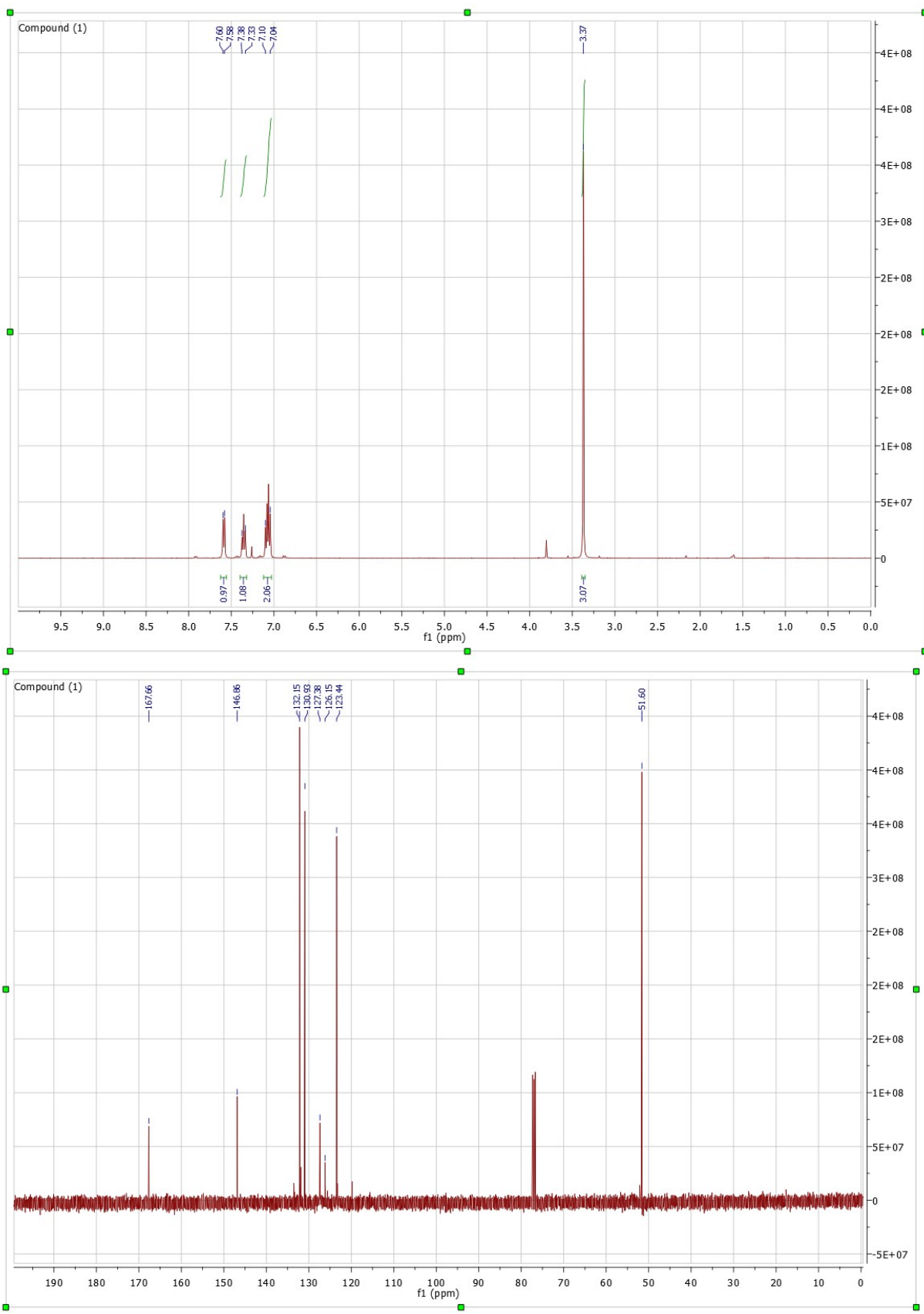


Figure S 21 - ^1H and ^{13}C NMR spectra of compound S3

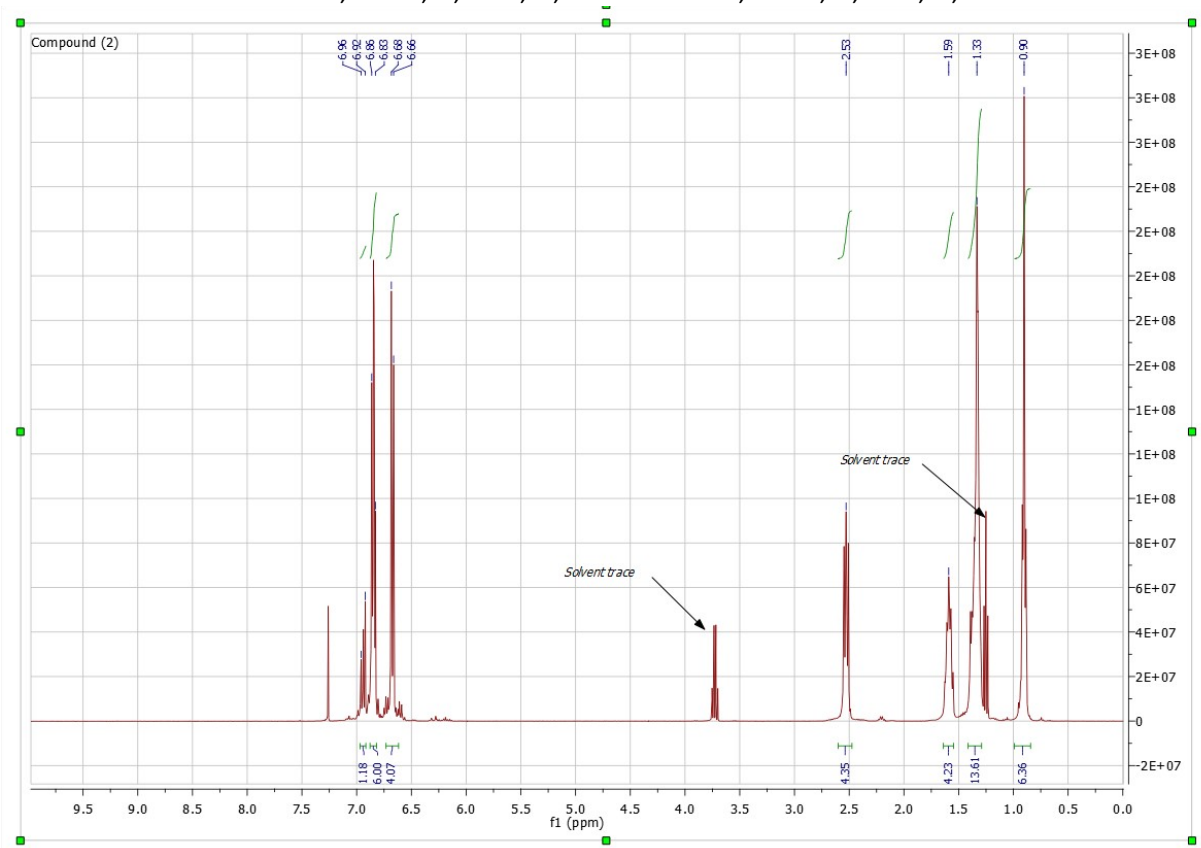
Synthesis of 4,4,8,8,12,12-hexakis(4-hexylphenyl)-8,12-dihydro-4H-benzo[9,1]quinolizino[3,4,5,6,7-defg]acridine (S4)

Under argon a dry round bottom flask was charged with 1(4-bromophenyl)hexane (2.0 g, 8.34 mmol) and 25 mL of freshly distilled THF. To this solution, n-BuLi (2.5 M in hexane, (3,7 mL, 9,18 mmol) at -78 °C was added slowly. The resulting mixture was allowed to stir at -78 °C for 30 min, and then a solution of the compound **S3** (500 mg, 1.19 mmol), in dry THF (10 mL) was added dropwise. The mixture was allowed to warm up to room temperature overnight. Then the reaction mixture was quenched with HCl (1 M) and extracted with ethyl ether. Combined organic phases were washed with brine, water and dried over Na₂SO₄, filtered and concentrated under vacuum. *p*-toluenesulfonic acid (615 mg, 3.58 mmol) and 50 mL of anhydrous toluene were added to the resulting oil, and was stirred at 80°C for 1h. A saturated NaHCO₃ aqueous solution was added and the mixture was extracted with diethyl ether and washed with water. The combined organic layers were dried over Na₂SO₄, filtered and concentrated under reduced pressure. The resulting oil was solubilized in a mixture of 10mL of dichloromethane and addition of 50 mL of ethanol precipitated the product. A white powder was collected by filtration and dried to afford the desired product **S4** as a white solid (1.12 g; 901 μmol, 75.6 %).

¹H NMR (400 MHz, CDCl₃, 298 K) δ 6.98 – 6.94 (m, 3H), δ 6.88 – 6.84 (m, 18H), δ 6.76 – 6.59 (m, 12H), δ 2.56 – 2.52 (m, 12H), δ 1.66 – 1.56 (m, 12H), δ 1.41 – 1.30 (m, 36H), δ 0.94 – 0.89 (m, 18H).

¹³C NMR (400 MHz, CDCl₃, 298 K) δ 143.8, δ 140.3, δ 135.2, δ 130.0, δ 128.7, δ 128.2, δ 127.3, δ 122.2, δ 55.3, δ 35.6, δ 31.8, δ 31.4, δ 29.3, δ 22.7, δ 14.1.

Anal. Calcd for C₉₃H₁₁₁N: C, 89.87; H, 9.00; N, 1.13. Found: C, 89.57; H, 8.84; N, 0.99.



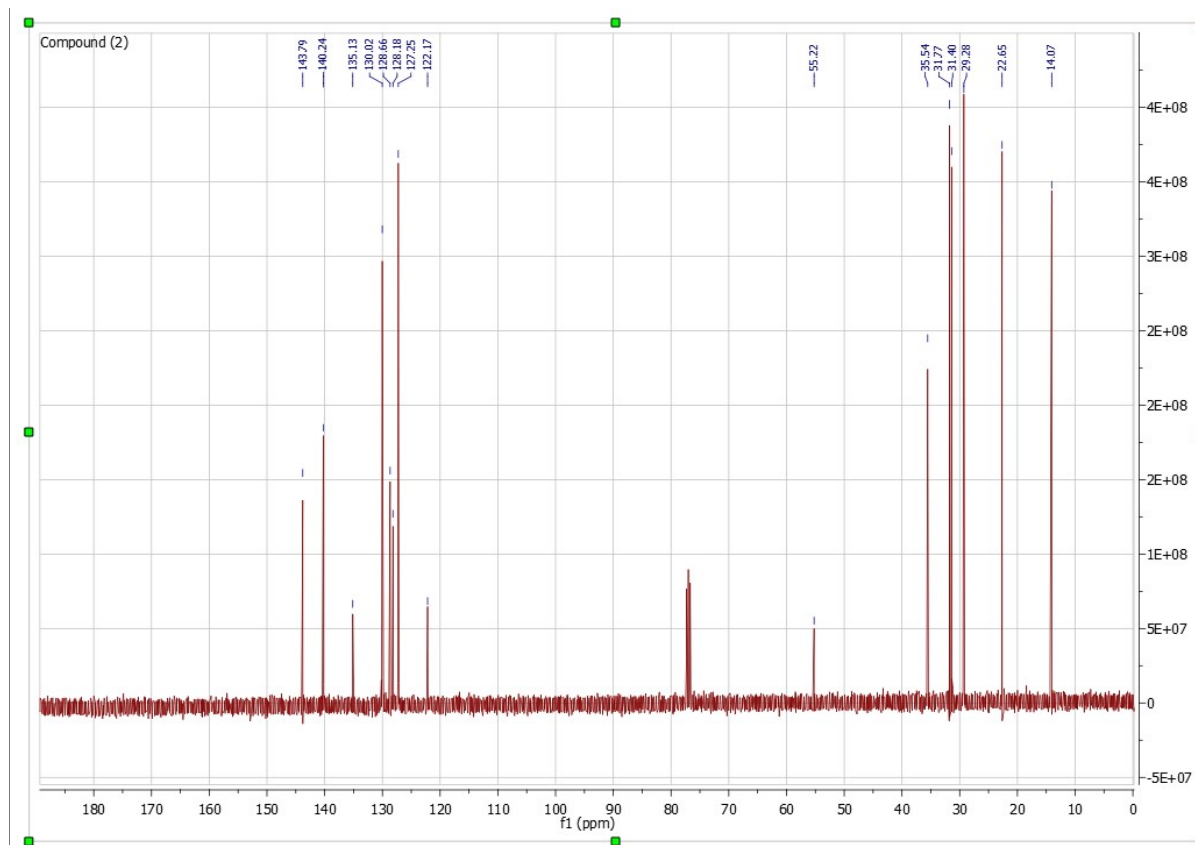


Figure S 22 - ^1H and ^{13}C NMR spectra of compound S4

Synthesis of 2,6,10-tribromo-4,4,8,8,12,12-hexakis(4-hexylphenyl)-8,12-dihydro-4H-benzo[9,1]quinolizino[3,4,5,6,7-defg]acridine (FTPA)

In a round bottom flask, compound **S4** (500mg, 402.3 μmol) was dissolved in chloroform (50 mL) and acetic acid (5 mL). *N*-bromosuccinimide (250 mg, 1.41mmol, 3.5 eq) was slowly added by portion at 0°C. The mixture was stirred for 1h and was allowed to warm up to room temperature overnight. The reaction was quenched with water, extracted with dichloromethane. The organic phase was dried over Na_2SO_4 , filtered and concentrated under reduced pressure. The residue was recrystallized in ethanol to obtain **FTPA** as a white crystals. (566 mg, 95.1%).

^1H NMR (400 MHz, CDCl_3 , 298 K) δ (ppm): 6.92 (s, 6 H), 6.88 (d, $J = 8.1$ Hz, 12 H), 6.59 (d, $J = 8.1$ Hz, 12 H), 2.56-2.52 (m, 12 H), 1.64- 1.58 (m, 12 H), 1.41-1.30 (m, 36 H), 0.94-0.89 (m, 18 H).

^{13}C NMR (400 MHz, CDCl_3 , 298 K) δ (ppm): 142.0, 141.2, 141.0, 133.9, 130.7, 130.5, 129.8, 127.7, 55.1, 35.5, 31.8, 31.3, 29.2, 22.7, 14.1.

Anal. Calcd for $\text{C}_{93}\text{H}_{108}\text{NBr}_3$: C, 75.49; H, 7.36; N, 0.95. Found: C, 75.62; H, 7.31; N, 0.84.

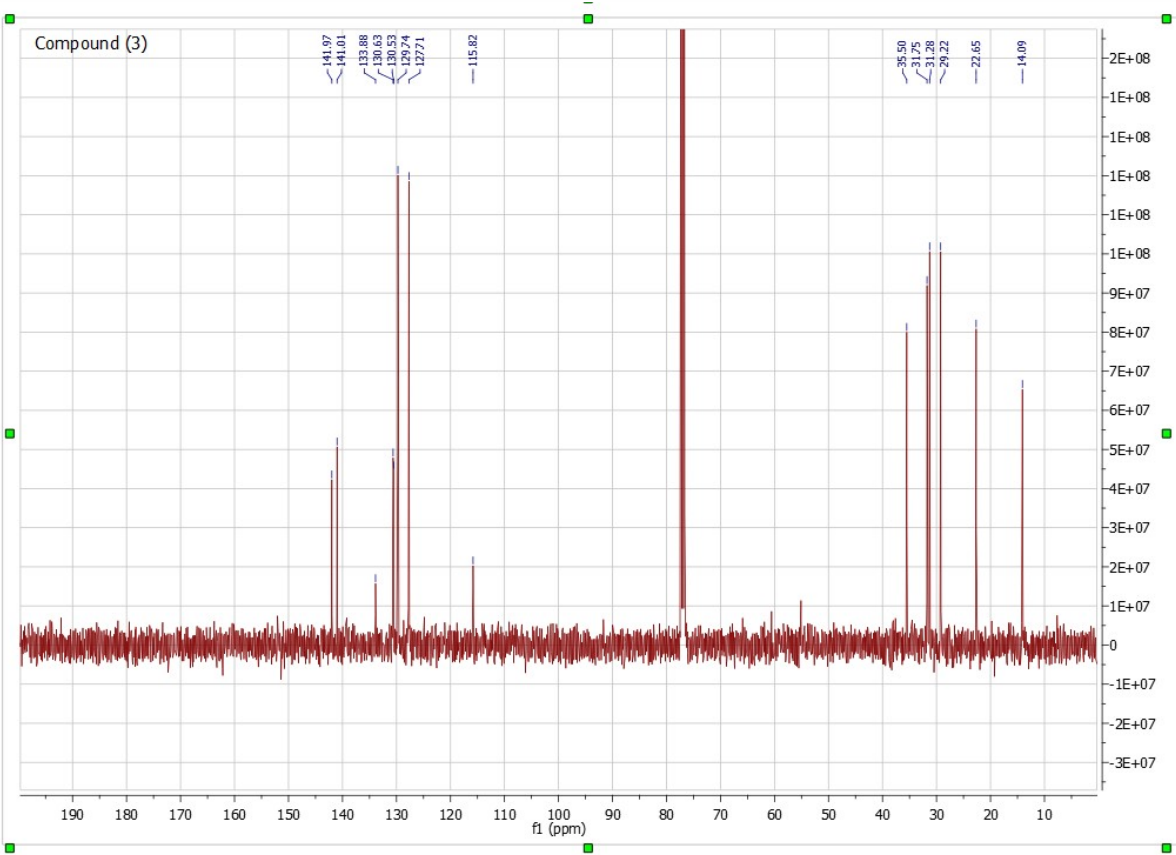
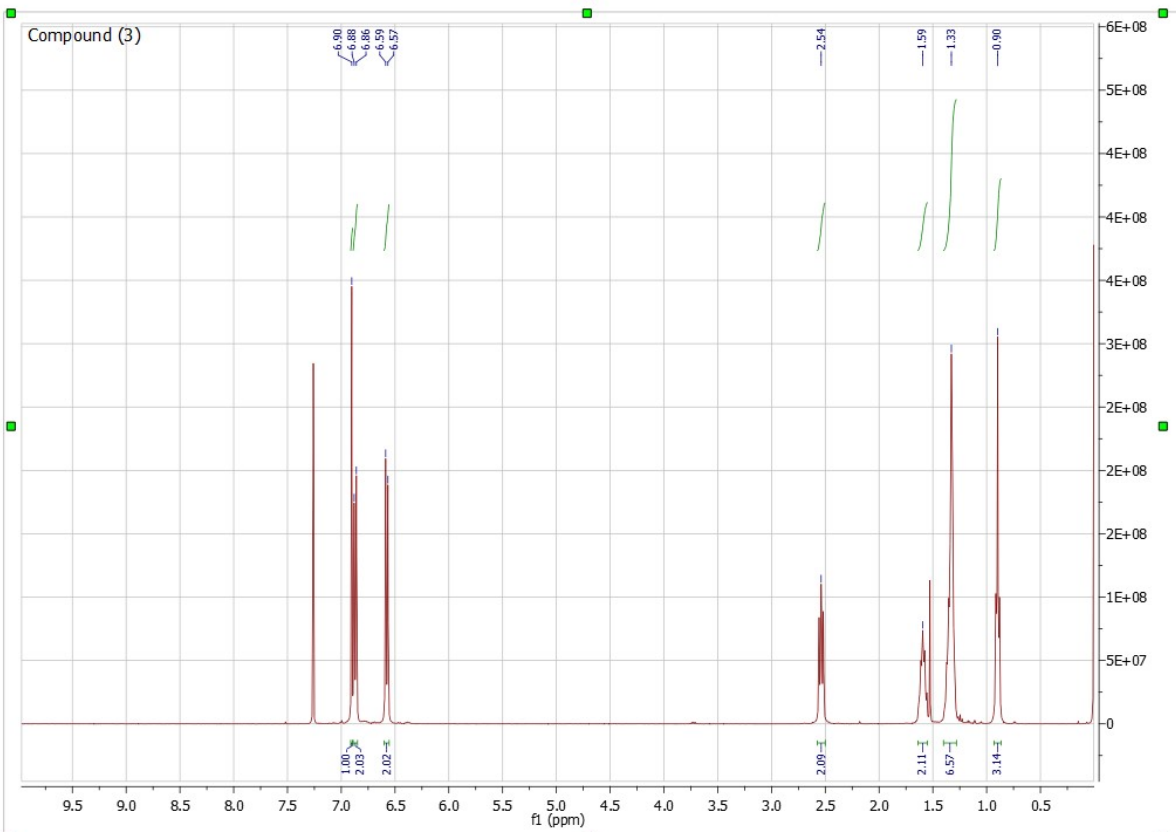


Figure S 23 - ¹H and ¹³C NMR spectra of compound FTPA

Synthesis of 5,5',5''-(4,4,8,8,12,12-hexakis(4-hexylphenyl)-8,12-dihydro-4H-

benzo[9,1]quinolizino[3,4,5,6,7-defg]acridine-2,6,10-triyl)tris(thiophene-2-carbaldehyde) (TriAld)

To a stirred solution of **S1** (570 mg, 2.87 mmol) in freshly distilled and degassed THF (25 mL), *n*-BuLi (2.5 M in hexane, 1.26 mL, 3.16 mmol, 1.10 eq) was added dropwise at -78°C. The reaction mixture was allowed to warm up to room temperature prior to the addition of tributyltin chloride (0.86 mL, 3.16 mmol, 1.10 eq) at -78°C. The mixture was stirred overnight at room temperature. Then, the mixture was poured into deionized water and extracted with diethyl ether. The organic layer was quenched with a saturated solution of ammonium chloride and with water and dried on Na₂SO₄, filtered and concentrated under vacuum. The resulting crude product (**S2**) was used in the next step without further purification. Under argon, compound **FTPA** (430 mg, 290.6 μmol), tris(dibenzylideneacetone) dipalladium(0) (32 mg, 34.9 μmol, 0.12 eq) and tri(*o*-tolyl)phosphine (21.2 mg, 69.7 μmol, 0.24 eq) were dried under vacuum for 30 min. The reactants were dissolved in anhydrous toluene (50 ml) and degassed prior heating at 80°C for 1h. Then a solution of **S2** (1.27 g, 2.62 mmol, 9 eq) in anhydrous toluene (20 mL) was added and the reaction mixture was refluxed overnight. The mixture was then poured into saturated aqueous NH₄Cl solution and the organic phase was extracted with Et₂O, washed with water, dried over Na₂SO₄ and concentrated. For aldehyde deprotection, the crude material was poured into a mixture of 40 mL of THF and 20 mL of HCl (6M) and refluxed for 3h. This organic solution was washed with a NaHCO₃ aqueous solution and water three times, dried over Na₂SO₄ and concentrated under vacuum. The crude solid was purified by flash chromatography using [*n*-hexane/chloroform 6:4] as eluent to afford **TriAld** as a yellow solid (403 mg, 88.1%).

¹H NMR (CDCl₃, 400 MHz, 298 K): δ (ppm) = 9.78 (s, 3H), 7.56 (d, *J* = 4.0 Hz, 3H), 7.20 (s, 6H), 6.92 (d, *J* = 8.5 Hz, 12H), 6.90 (d, *J* = 4.0 Hz, 3H), 6.71 (d, *J* = 8.3 Hz, 12H), 2.58 (m, 12H), 1.62 (m, 12H), 1.34 (m, 36H), 0.90 (m, 18H).

¹³C NMR (CDCl₃, 100 MHz, 298 K): δ (ppm) = 182.48, 154.14, 142.26, 141.63, 141.18, 137.40, 135.13, 129.88, 129.83, 127.83, 127.73, 126.03, 123.06, 55.32, 35.48, 31.75, 31.28, 29.14, 22.68, 14.11.

Anal. Calcd for C₁₀₈H₁₁₇NO₃S₃: C, 82.45; H, 7.50; N, 0.89, S, 6.11. Found: C, 81.86; H, 7.32; N, 0.67, S, 5.89.

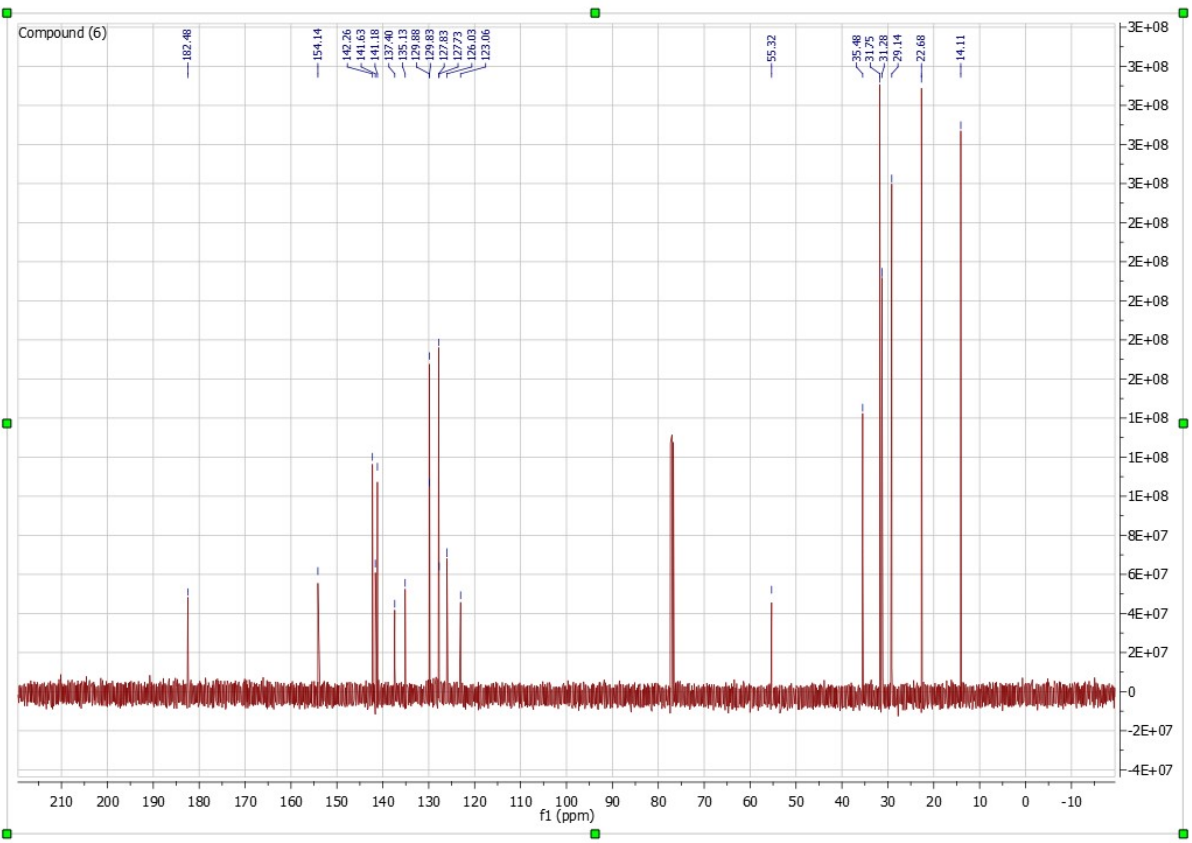
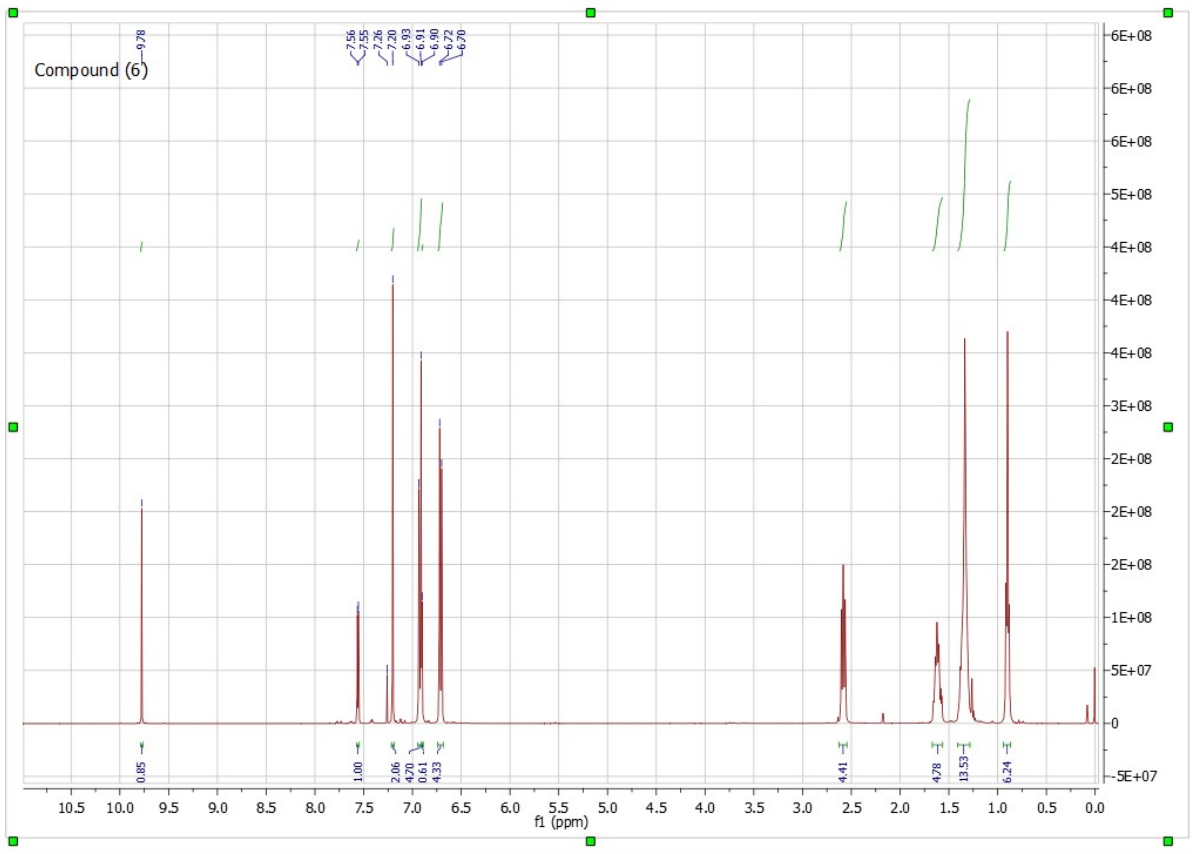


Figure S 24 - ^1H and ^{13}C NMR spectra of compound TriAld

Synthesis of AzaTk

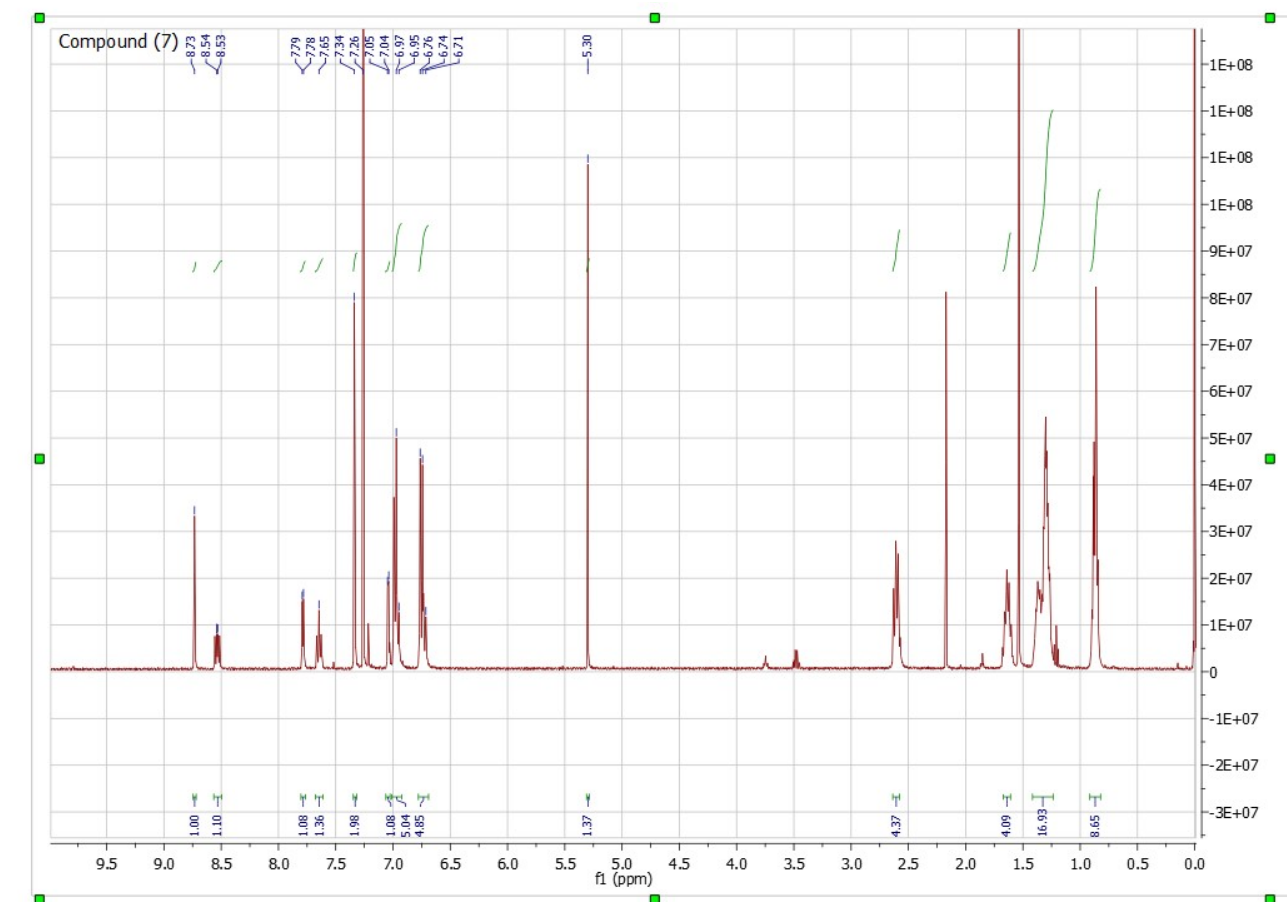
Compound **TriAld** (200 mg, 127.1 μmol) and 2-(5,6-difluoro-3-oxo-2,3-dihydro-1*H*-inden-1-ylidene)malononitrile (204.8 mg, 889.8 μmol , 7 eq) were dried under vacuum for 1h in a round-bottom flask. Then, 10 mL of a [CHCl_3 :pyridine : 95:5 ,v/v] solution was injected and the solution was stirred 5h at 70°C. The mixture was allowed to cool down at room temperature and the crude product was precipitated in cold methanol (250mL). The resulting dark solid was filtered and then purified by column chromatography on silica using [*n*-hexane/chloroform 1:1] as eluent to afford **AzaTk** as a dark blue solid (238 mg, 84.7%).

$^1\text{H NMR}$ (CDCl_3 , 400 MHz, 298 K): δ (ppm) = 8.73 (s, 3H), 8.53 (dd, $J = 9.8, 6.6$ Hz, 3H), 7.79 (d, $J = 4.1$ Hz, 3H), 7.65 (t, $J = 7.4$ Hz, 3H), 7.34 (s, 6H), 7.05 (d, $J = 4.0$ Hz, 3H), 7.02 – 6.93 (m, 15H), 6.78 – 6.70 (m, 15H), 5.30 (s, 3H), 2.64 – 2.58 (m, 12H), 1.67 – 1.61 (m, 12H), 1.42 – 1.24 (m, 36H), 0.88 (m, 18H).

$^{13}\text{C NMR}$ (CDCl_3 , 100 MHz, 298 K): δ (ppm) = 185.45, 161.12, 158.49, 155.74, 153.22, 153.12, 146.62, 141.93, 141.87, 141.49, 137.93, 136.53, 135.98, 135.65, 134.59, 130.44, 129.88, 128.16, 127.99, 126.55, 124.78, 121.45, 115.09, 114.88, 114.20, 114.03, 112.61, 112.42, 69.98, 55.38, 35.57, 31.79, 31.39, 29.28, 29.25, 22.70, 14.09.

$^{19}\text{F NMR}$ (CDCl_3 , 376 MHz, 298 K): δ (ppm) = -122.60 (m, 1F), -123.76 (m, 1F)

HRMS (MALDI): calcd. for $\text{C}_{144}\text{H}_{123}\text{N}_7\text{O}_3\text{F}_6\text{S}_3$, 2207.875; found 2207.880 (2 ppm).



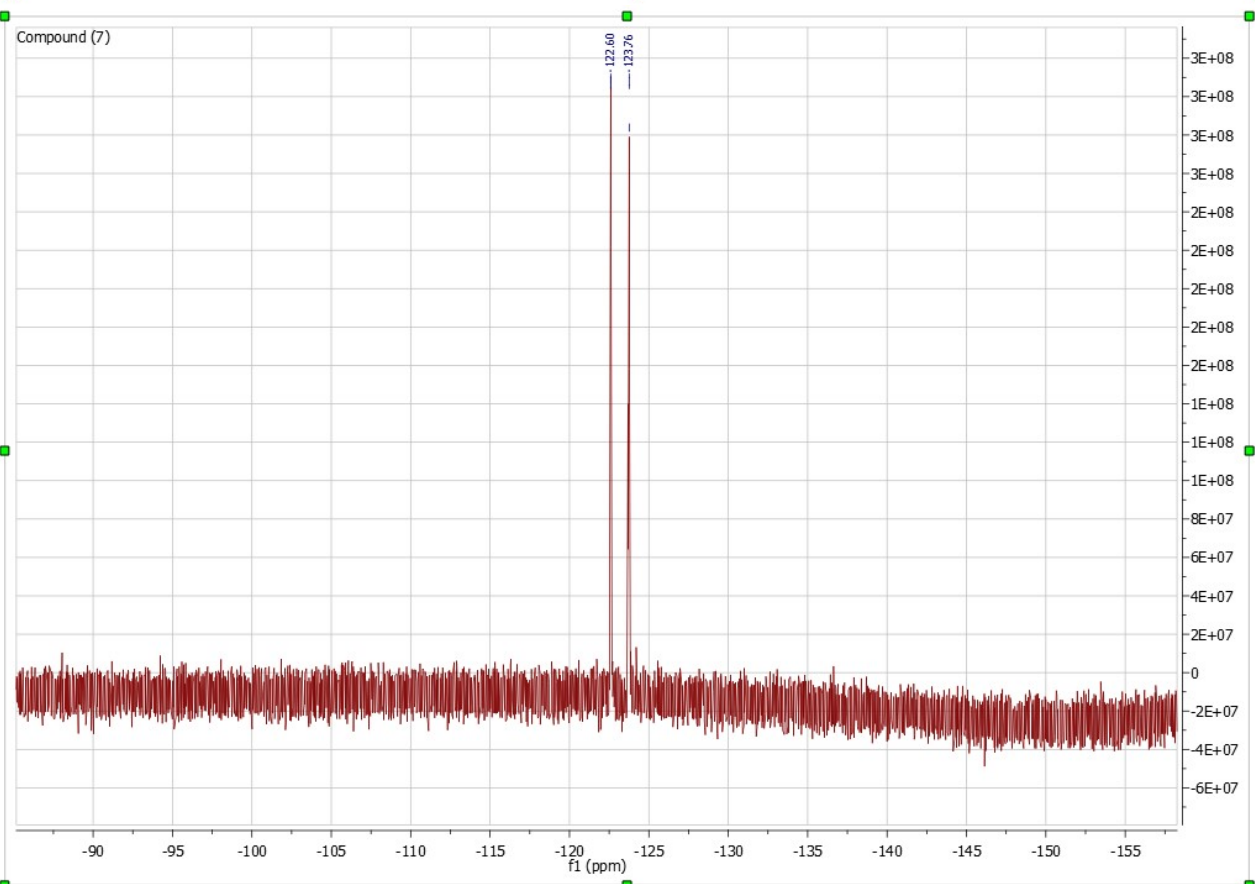
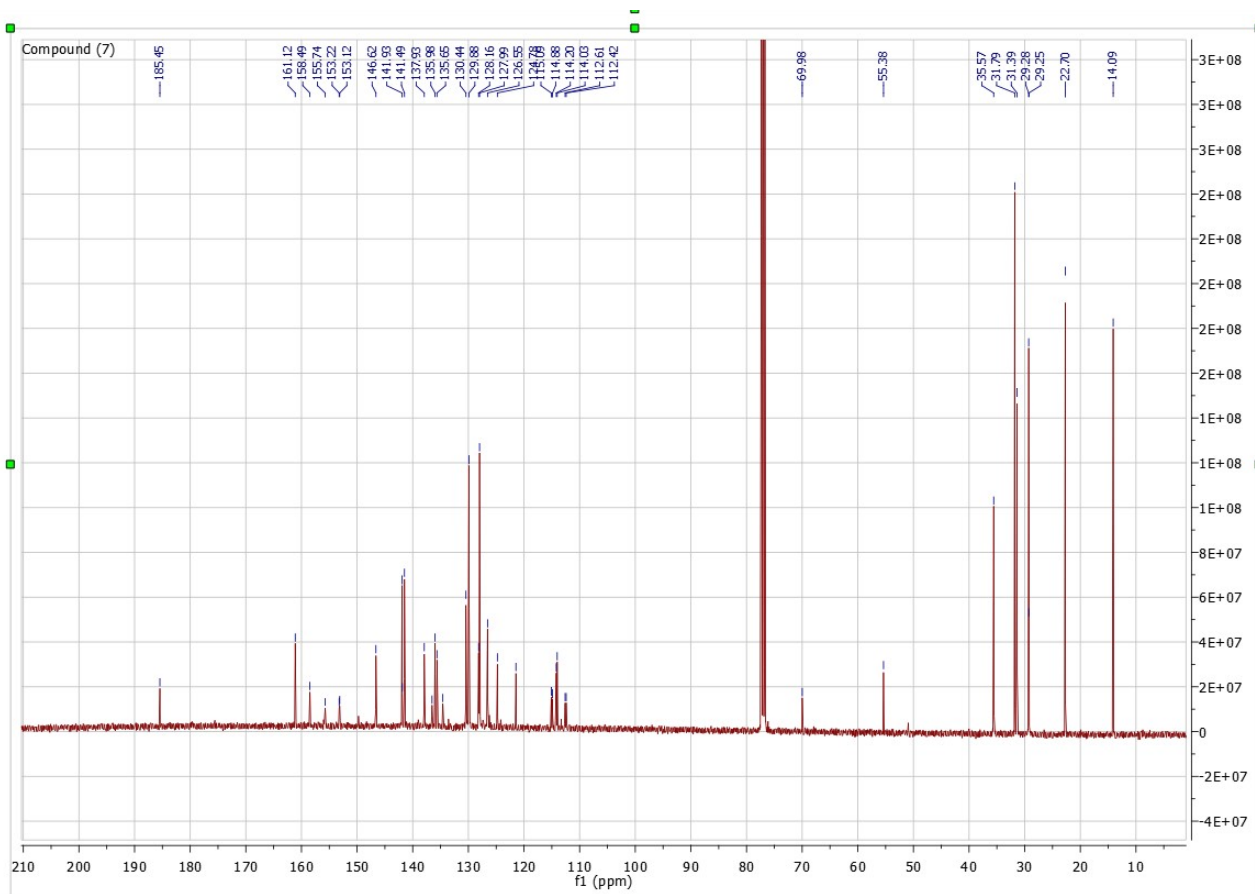


Figure S 25 - ^1H , ^{13}C and ^{19}F NMR spectra of compound AzaTk

VI. Xray Crystallographic structure datas

AzaTk Crystal :

Experimental. Single lustrous dark red prism-shaped crystals of **AzaTk** were obtained by recrystallisation from dibromomethane/cyclohexane mixture. A suitable crystal 0.50×0.25×0.06 mm³ was selected and mounted on a suitable support on an Xcalibur, Sapphire3 diffractometer. The crystal was kept at a steady $T = 149.95(10)$ K during data collection. The structure was solved with the ShelXT n/a (Sheldrick, 2015) structure solution program using the Intrinsic Phasing solution method and by using **Olex2** (Dolomanov et al., 2009) as the graphical interface. The model was refined with version 2018/3 of ShelXL 2018/3 (Sheldrick, 2015) using Least Squares minimisation.

Crystal Data. C₁₄₄H₁₂₃F₆N₇O₃S₃, $M_r = 2209.67$, triclinic, $P-1$ (No. 2), $a = 17.8524(8)$ Å, $b = 19.0237(11)$ Å, $c = 20.7805(11)$ Å, $\alpha = 108.559(5)^\circ$, $\beta = 106.629(4)^\circ$, $\gamma = 107.455(5)^\circ$, $V = 5786.2(6)$ Å³, $T = 149.95(10)$ K, $Z = 2$, $Z' = 1$, $\mu(\text{Mo K}\alpha) = 0.134$, 51412 reflections measured, 19417 unique ($R_{\text{int}} = 0.1169$) which were used in all calculations. The final wR_2 was 0.3207 (all data) and R_1 was 0.0985 ($I > 2(I)$).

FTPA Crystal:

Experimental. Single crystals of C₉₃H₁₀₈Br₃N [**S4**] were **recrystallized from hexane**. A suitable crystal was selected and mounted on a **Xcalibur, Sapphire3** diffractometer. The crystal was kept at 149(2) K during data collection. Using Olex2 [1], the structure was solved with the ShelXT [2] structure solution program using Direct Methods and refined with the ShelXL [3] refinement package using Least Squares minimisation.

Crystal Data for C₉₃H₁₀₈Br₃N (M = 1479.53 g/mol): monoclinic, space group P2₁/c (no. 14), $a = 16.5370(6)$ Å, $b = 24.2725(9)$ Å, $c = 18.8997(8)$ Å, $\beta = 90.478(3)^\circ$, $V = 7586.0(5)$ Å³, $Z = 4$, $T = 149(2)$ K, $\mu(\text{MoK}\alpha) = 1.643$ mm⁻¹, $D_{\text{calc}} = 1.295$ g/cm³, 68701 reflections measured ($3.666^\circ \leq 2\theta \leq 52.742^\circ$), 15527 unique ($R_{\text{int}} = 0.1843$, $R_{\text{sigma}} = 0.1704$) which were used in all calculations. The final R_1 was 0.0760 ($I > 2\sigma(I)$) and wR_2 was 0.1342 (all data).

S4 Crystal :

Experimental. Single crystals of C₉₃H₁₀₈Br₃N [**S4**] were **recrystallized from hexane**. A suitable crystal was selected and mounted on a **Xcalibur, Sapphire3** diffractometer. The crystal was kept at 149(2) K during data collection. Using Olex2 [1], the structure was solved with the ShelXT [2] structure solution program using Direct Methods and refined with the ShelXL [3] refinement package using Least Squares minimisation.

Crystal Data for C₉₃ H₁₁₁ N (M = 1242.82g/mol): Monoclinic Space group P 21/c Unit cell dimensions $a = 21.5377(15)$ Å $\alpha = 90$ deg. $b = 21.122(2)$ Å $\beta = 108.215(7)$ deg. $c = 17.1592(11)$ Å $\gamma = 90$ deg. Volume, $Z = 4$ Density (calculated) 1.113 g/cm³ Absorption coefficient 0.062 mm⁻¹ $F(000) = 2704$ Crystal size 1.1910 x 0.6484 x 0.2193 mm Theta range for data collection 3.119 to 26.372 deg. Limiting indices $-26 \leq h \leq 26$, $-26 \leq k \leq 20$, $-21 \leq l \leq 18$ Reflections collected 34459 Independent reflections 15123 [$R_{\text{int}} = 0.0691$] Absorption correction Analytical Max. and min. transmission 0.986 and 0.960 Refinement method Full-matrix least-squares on F^2 Data / restraints / parameters 15123 / 30 / 938 Goodness-of-fit on F^2 1.031 Final R indices [$I > 2\sigma(I)$] $R_1 = 0.0859$, $wR_2 = 0.1832$ R indices (all data) $R_1 = 0.1786$, $wR_2 = 0.2360$

References:

[1] Y. A. Avalos-Quiroz, T. Koganezawa, P. Perkhun, E. Barulina, C.M. Ruiz, J. Ackermann, N. Yoshimoto, C. Videlot-Ackermann. *Adv. Electron. Mat.*, 2022, 8 (3), 2100743.

- [2] Y. A. Avalos-Quiroz, O. Bardagot, Y. Kervella, C. Aumaître, L. Cabau, A. Rivaton, O. Margeat, C. Videlot-Ackermann, U. Vongsaysy, J. Ackermann, R. Demadrille. *ChemSusChem*, 2021, 14, 3502-3510.
- [3] S. Ben Dkhil, P. Perkhun, C. Luo, D. Müller, R. Alkarsifi, E. Barulina, Y.A. Avalos Quiroz, O. Margeat, S.T. Dubas, T. Koganezawa, D. Kuzuhara, N. Yoshimoto, C. Caddeo, A. Mattoni, B. Zimmermann, U. Würfel, M. Pfannmöller, S. Bals, J. Ackermann, C. Videlot-Ackermann. *ACS Appl. Mater. Interfaces* 2020, 12, 28404-28415.